

PML-Nuclear Body Dynamics in Canine Parvovirus Infection



Juha Laurila

Undergraduate Thesis

University of Jyväskylä

Department of Biological and Environmental Science

April 2007

PREFACE

This work was executed in 2005-2006, at the section of molecular biology, department of biological and environmental science, University of Jyväskylä.

I would like to express my deepest gratitude to MSc Teemu Ihalainen for his excellent supervision, as well as the group leader, PhD Maija Vihinen-Ranta, for the opportunity to work in such an interesting project. In addition, not to underestimate the effect of the working environment, I want to thank everyone in the lab for the good atmosphere.

I also want to thank my family and of course Timo, Maija and Olli for their support during this lengthy project.

In Turku, April 19th, 2007

Juha Laurila

Tekijä: Juha Laurila
Tutkielman nimi: PML-tumarakenteiden dynamiikka koiran parvovirusinfektiossa
English title: PML-Nuclear Body Dynamics in Canine Parvovirus Infection
Päivämäärä: 19.4.2007 **Sivumäärä:** 61

Laitos: Bio- ja ympäristötieteiden laitos
Oppiaine: Molekyylibiologia
Tutkielman ohjaaja(t): Teemu Ihalainen, Maija Vihinen-Ranta

Tiivistelmä:

Koiran parvovirus (CPV, Canine Parvovirus) on hyvin pieni virus, halkaisijaltaan vain noin 26Å. Koiran parvoviruksen genomi on yksijuosteista DNA:ta, pituudeltaan 5,3 kiloemästä. Pienen kokonsa takia koiran parvovirus on erittäin riippuvainen isäntäsolustaan. Useimpien muiden DNA-virusten tavoin koiran parvovirus lisääntyy isäntäsolun tumassa. Promyelosyyttisen leukemia (PML)-proteiinin löytyminen on seurausta sen yhteydestä harvinaiseen, mutta erittäin vaaralliseen akuuttiin promyelosyyttiseen leukemiaan. Myöhemmin PML-proteiini on paljastunut mahdolliseksi uudelleenlaiseksi virusinfektiota vastaan taistelevaksi tekijäksi. Sen ilmentyminen lisääntyy seurauksena tyypin II interferoneille, joita perinteisesti pidetään merkittävimpinä solun puolustusmekanismeina viruksia vastaan. PML-proteiini on tumassa keskittynyt tiettyihin rengasmaisiin rakenteisiin, joita kutsutaan mm. nimillä PML-tumarakenne (PML-NB), PML onkogeenninen piste (POD), Kramer rakenne tai tuma domeeni 10 (ND10). PML-tumarakenteet ovat dynaamisia, ja ne reagoivat solua uhkaaviin stressitekijöihin. PML-tumarakenteiden todellinen merkitys soluille on kuitenkin edelleen kiistanalainen. Useiden virusten, koiran parvovirus mukaan luettuna, voidaan havaita löytyvän läheltä PML-tumarakenteita infektion aikana, ne ovat myös kehittäneet useita menetelmiä hajottaa PML-tumarakenteet. Virusten ja PML-tumarakenteiden läheisyyden merkityksestä löytyy ristiriitaisia todisteita. Tässä tutkimuksessa me käytimme hyväksi konfokaalimikroskopiaa tutkiaksemme koiran parvoviruksen vaikutusta PML-tumarakenteiden dynamiikkaan. Hyödynsimme erityisesti kahta menetelmää: valkaisun jälkeistä fluoresenssin palautumista (FRAP, Fluorescence recovery after photobleaching) ja 4-ulotteista (4D) kuvantamista. Koiran parvoviruksella ei havaittu olevan tilastollisesti merkittävää vaikutusta: PML-tumarakenteiden keskikoko, -lukumäärä ja -nopeus, olivat kaikki likimäärin samoja infektoiduissa ja infektoimattomissa soluissa ($p=0,166$, $p=0,389$ and $p=0,113$). Yli 50 nm/s liikkuvien PML-tumarakenteiden lukumäärä oli kuitenkin hieman koholla infektoiduissa soluissa ($p=0,052$), mikä on erittäin lievä vaikutus verraten monien muiden virusten aikaansaannoksiin. Koiran parvoviruksella ei näytä olevan tarvetta hajottaa PML-tumarakenteita. Tämä voi viitata siihen, että CPV ei ole altis PML:n välittämälle viruspuolustukselle, tai kykenee välttämään sen vielä tuntemattomalla tavalla. PML-tumarakenteiden rooli CPV-infektiossa voi olla myös täysin toinen, nimittäin viruksen monistuminen. Seurasimme CPV:n sijaintia leimaamalla viruksen proteiini NS1, joka on mielenkiintoista kyllä viruksen monistumiselle välttämätön proteiini. FRAP:lla osoitimme PML IV-proteiinin olevan vapaasti liikkuva, vaikkakin 158 sekunnin palautumisen puoliaika (t_D) viittaa varsin tiukkaan sitoutumiseen. Perusteellista data-analyysiä vaikeutti kuitenkin liian voimakas valkaisu.

Avainsanat: Koiran parvovirus, CPV, Promyelosyyttinen leukemia tumarakenne, PML, viruspuolustus, valkaisun jälkeinen fluoresenssin palautuminen, FRAP, 4D kuvantaminen

Author: Juha Laurila
Title of thesis: PML-Nuclear Body Dynamics in Canine Parvovirus Infection
Finnish title: PML-tumarakenteiden dynamiikka koiran parvovirusinfektiossa
Date: 19.4.2007 **Pages:** 61

Department: Department of Biological and Environmental Science
Chair: Molecular Biology
Supervisor(s): Teemu Ihalainen, Maija Vihinen-Ranta

Abstract:

Canine parvovirus (CPV) is roughly 26Å in diameter and has a 5.3kb long single-stranded DNA genome. The very small genome subdues CPV strongly dependent on nuclear processes of the host cell, requiring actively dividing cells to replicate. Like most other DNA viruses, CPV replicates within the host cell nucleus. Promyelocytic leukaemia (PML) protein, found due to its involvement in acute promyelocytic leukaemia (APL), is a novel component postulated to participate in the cellular anti-viral defence. Its expression is induced in response to type II interferons, a major defence line against viral infections. PML is the defining constituent of nuclear structures known as nuclear domain 10 (ND10), Kramer bodies, PML oncogenic dots (POD) or simply PML nuclear bodies (PML-NB). PML-NBs are dynamic structures known to respond to cellular stress, but whose exact function has been under rigorous debate. Nonetheless, many viruses, including CPV, are localized near PML-NBs in the course of infection and viruses have evolved diverse methods to disrupt PML-NBs. However, evidence for the significance of the virus-PML-NB co-localization is in some part contradictory. Here, we describe the use of confocal microscopy to define the effect of CPV infection on PML-NB dynamics. Two methods are emphasized in particular: fluorescence recovery after photobleaching (FRAP) and four-dimensional (4D) imaging. CPV appeared to have no significant effect on PML-NB dynamics. Average number, size and speed, all remained roughly the same in infected cells ($p=0.166$, $p=0.389$ and $p=0.113$, respectively). A borderline insignificant increase in the amount of PML-NBs moving over 50nm/s was however revealed ($p=0.052$), a very mild response considering what other viruses are capable of. The lack of significant effect may suggest CPV not being susceptible for PML-mediated anti-viral effects, or circumventing them by yet unknown mechanism. It may also hint for another role for PML-NBs in CPV infection, i.e. that of viral replication. It is the NS1 protein, important factor in viral replication, that was followed to the PML-NBs. Using FRAP we showed PML IV to be fully mobile within the nucleus, although the half time of recovery (t_D) of 158 seconds suggests rather tight binding interactions. Thorough data analysis was hindered however by too intense bleaching.

Keywords: Canine parvovirus, CPV, Promyelocytic leukaemia nuclear body, PML-NB, anti-viral defence, FRAP, Fluorescent recovery after photobleaching, 4D imaging

TABLE OF CONTENTS

<u>PREFACE.....</u>	<u>2</u>
<u>ABSTRACTS.....</u>	<u>3</u>
<u>ABBREVIATIONS</u>	<u>7</u>
<u>INTRODUCTION.....</u>	<u>8</u>
CANINE PARVOVIRUS	9
EVOLUTION	9
THE FAMILY TREE.....	10
STRUCTURAL FEATURES	10
SNEAKING BY THE CELL MEMBRANE	13
TOWARDS THE NUCLEUS	15
VIRAL REPLICATION	16
THE GRAND WALKOUT	17
THE PATHOGENESIS	18
PROMYELOCYTIC LEUKAEMIA NUCLEAR BODIES.....	19
CELL VS. VIRUS.....	19
NUCLEAR SUBSTRUCTURE OF MAMMALIAN CELL NUCLEUS.....	20
PML PROTEIN.....	21
PML-NBS – STRUCTURE AND DYNAMICS	23
FUNCTION.....	26
CONFOCAL MICROSCOPY	29
GREEN FLUORESCENT PROTEIN	29
OPERATIONAL PRINCIPLE OF CONFOCAL MICROSCOPE	30
CLSM – A VERSATILE TOOL.....	31
FRAP – A CLOSER LOOK	35
QUANTITATIVE CONFOCAL MICROSCOPY – IN CONCLUSION.....	37
<u>AIM OF THE STUDY.....</u>	<u>38</u>

<u>MATERIALS AND METHODS</u>	39
SAMPLE PREPARATION	39
PLASMIDS	39
CELL CULTURE AND TRANSFECTIONS.....	39
VIRUSES AND INFECTION	40
IMMUNOFLUORESCENT LABELLING.....	40
CONFOCAL MICROSCOPY	40
EQUIPMENT	40
PERFORMING FRAP EXPERIMENTS AND ANALYSIS OF THE DATA ACQUIRED.....	41
MOVEMENT OF THE PML-NBS AND ANALYSIS OF THE DATA ACQUIRED	42
<u>RESULTS</u>	43
CANINE PARVOVIRUS CO-LOCALIZES WITH PML-NUCLEAR BODIES WITHIN 12 HOURS OF INFECTION	43
CANINE PARVOVIRUS APPEARS TO HAVE VERY LITTLE EFFECT ON PML NUCLEAR BODY DYNAMICS UPON INFECTION.....	44
DYNAMIC PROPERTIES OF PML-PROTEIN REMAIN UNAFFECTED IN CPV INFECTION.....	45
<u>DISCUSSION</u>	46
CPV – PML INTERACTION	46
EXECUTION OF FRAP.....	48
FINALLY,	49
<u>REFERENCES</u>	50

ABBREVIATIONS

AAV	Adeno-Associated Virus
APL	Acute Promyelocytic Leukaemia
ATRA	All-trans Retinoic Acid
CFP	Cyan Fluorescent Protein
CLSM	Confocal Laser Scanning Microscope
CPV	Canine Parvovirus
D	Diffusion Coefficient
eIF2	Eukaryotic Initiation Factor 2
FLIM	Fluorescence Lifetime Imaging Microscopy
FLIP	Fluorescence Loss In Photobleaching
FPV	Feline Panleukopenia Virus
FRAP	Fluorescence Recovery After Photobleaching
FRET	Fluorescence Resonance Energy Transfer
GFP	Förster Resonance Energy Transfer
HCMV	Green Fluorescent Protein
HIV	Human Cytomegalovirus
HSV-1	Human Immunodeficiency Virus
IFN	Herpes Simplex Virus-1
M _f	Interferon
MOI	Mobile Fraction
MVM	Multiplicity of Infection
ND10	Minute Virus of Mouse
NLFK	Nuclear Domain 10
NLS	Norden Laboratories Feline Kidney
NPC	Nuclear Localization Signal
NS1 and NS2	Nuclear Pore Complex
OAS	Nonstructural Proteins 1 and 2
ORF	(2'-5')-Oligoadenylatesynthetase
P4 and P38	Open Reading Frame
PKR	Promoters 4 and 38
PLA ₂	dsRNA-Dependent Protein Kinase
PML-NB	Phospholipase A ₂
POD	Promyelocytic Leukaemia Nuclear Body
PPV	PML Oncogenic Dot
pRB	Porcine Parvovirus
RAR	Retinoblastoma Protein
RFP	Retinoic Acid Receptor
RING domain	Red Fluorescent Protein
ROI	Really Interesting New Gene domain
RPA	Region of Interest
SUMO	Replication Protein A
T _{1/2} or T _D	Small Ubiquitin-Like Modifier
TfR	Halftime of Recovery
TRIM	Transferrin Receptor
VP1, VP2 and VP3	Tripartite Motif
YFP	Viral Proteins 1, 2 and 3
	Yellow Fluorescent Protein

Introduction

Canine parvovirus (CPV) belongs to a family of viruses that possess a unique feature of linear single-stranded (ss) DNA genome. Very small linear ssDNA genome forces parvoviruses under strict dependence on the processes of the host cell. Although the virus harbours only a few proteins of its own, they accomplish a multitude of viral functions by carrying several functional activities. Since its emergence in the late 1970s, canine parvovirus has become a widespread epidemic among dogs. Although CPV has been under extensive study since its emergence, more is known of some of its relatives like minute virus of mouse or the adeno-associated viruses.

As a cell is exposed to viral infection it may take drastic measures to defend itself and to notify surrounding cells of the problems it is facing. The type I interferon (IFN) response is considered as the primary reaction against viral infection, but novel mechanisms have been discovered in recent years. Some of the recently discovered anti-viral mechanisms involve nuclear and cytoplasmic proteins belonging to the tripartite motif (TRIM) protein family, a member of this family is known as Promyelocytic leukaemia (PML) protein. Promyelocytic leukaemia protein is a major constituent of nuclear structures known as nuclear domain 10 (ND10), Kramer bodies, PML oncogenic dots (POD) or simply PML nuclear bodies (PML-NB), used hereafter. The PML-NBs are only one of many subnuclear organelles discovered. The PML-NBs are dynamic structures and their function has proven to be difficult to define as they contain several proteins taking part in divergent nuclear processes. Among many other postulated functions, PML-NBs have been linked to type I interferon response and thus, the anti-viral defence.

Among the methods used to study dynamics of nuclear proteins and organelles are fluorescence recovery after photobleaching (FRAP) and four-dimensional (4D) imaging, both executed using confocal microscope. Confocal laser scanning microscope (CLSM) is a versatile tool to which many research methods has been developed. Images obtained with CLSM may be impressive but quantitative data is required to ensure reliable conclusions, many mathematical models are available for this purpose.

Canine Parvovirus

Evolution

A new canine virus emerged in 1978 to wreak havoc among dogs in several countries around the world. In less than four years some of the structural features of the virus were already known and the virus was classified as a *canine parvovirus* (CPV) (Paradiso, P.R. et al., 1982). In 1985 the nucleotide sequence of the gene coding for capsid proteins VP1 and VP2 (viral proteins 1 and 2) was determined (Rhode, S.L., 3rd, 1985a) and three years later the whole genome sequence of CPV was elucidated (Reed, A.P. et al., 1988). Atomic structures of the DNA-containing and empty CPV capsids were published in the early 1990s with resolutions of 3.25Å and 3.0Å, respectively (Tsao, J. et al., 1991, Wu, H., and Rossmann, M.G., 1993), and in 1996 the structure of DNA-containing capsid was refined to 2.9Å (Xie, Q., and Chapman, M.S., 1996).

The emergence of CPV in such a near past provides an excellent opportunity to study host-range shift and virus-host interaction. CPV emerged by a host-range shift of feline panleukopenia virus (FPV) (Siegl, G. et al., 1985). Change in only five amino acid residues of the viral protein 2 (VP2) is sufficient to cause the shift of FPV host-range from cats to dogs. Change of the residues 93 and 323 led to capability of the virus to bind canine transferrin receptor (TfR) (Hueffer, K. et al., 2003), while change of residues 80, 564 and 568 is thought to have lead to loss of feline host-range (Truyen, U. et al., 1996). The original CPV strain named type 2 was replaced by strains 2a and 2b in only two years. Strains 2a and 2b reclaimed the ability to infect cats in addition to dogs (Truyen, U. et al., 1996). The CPV and FPV host-ranges are rather unclear and may differ *in vivo* and *in vitro* (Truyen, U., and Parrish, C.R., 1992), *in vivo*, CPV has been found to infect coyotes and domestic cats and dogs (Truyen, U. et al., 1996) while FPV infects raccoons, minks and cats (Barker, I.K. et al., 1983).

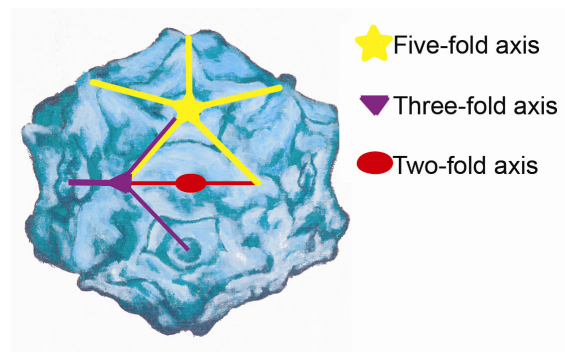
For rapidly evolving RNA viruses, evolution ensues high nucleotide substitution rate caused partly by lack of proofreading activity of the RNA-dependent RNA-polymerases (For review see Reaney, D.C., 1982). In contrast, it is assumed that double-stranded (ds) DNA viruses have a rate of nucleotide substitution not far from their hosts, due to their use of cellular enzymes to replicate. However, few estimates of rate of nucleotide substitution for single-stranded DNA viruses are available. One such shows that CPV has a nucleotide substitution rate close to that of RNA viruses like HIV-1 or influenza A. High nucleotide substitution rate has made it possible for CPV to generate a number of antigenic and host-range variants during its relatively short existence (Shackelton, L.A. et al., 2005).

The Family Tree

Canine parvovirus belongs to genus *parvoviruses*, one of the five genera of the subfamily *parvovirinae*, four other genera being *erythro-*, *dependo-*, *amdo-* and *bocaviruses*. All but *dependoviruses* are capable of infecting target cells independently, whereas *dependoviruses* require a concurrent infection, typically by an adenovirus, to multiply. For this reason many of the dependoviruses are named adeno-associated viruses (AAV). The subfamily *parvovirinae* forms the virus family *parvoviridae* along with the subfamily *densovirinae*. Members of the family *parvoviridae* are among the smallest of the DNA animal viruses and are the only known viruses with linear single-stranded DNA genome. *Parvovirinae* is a group of vertebrate infecting viruses, whereas members of the subfamily *densovirinae* infect invertebrates.

Structural Features

Fig 1. The structure of CPV capsid. The CPV capsid displays icosahedral symmetry with triangulation number 1, as determined by Caspar and Klug (CASPAR, D.L., and KLUG, A., 1962). The capsid is constructed of 60 copies of capsid proteins, of which VP2 is the main constituent. Three types of axes of rotational symmetry can be recognized from the structure: five-, three- and two-fold.



Canine parvovirus is a non-enveloped, single-stranded (ss) DNA virus, roughly 26nm in diameter with a capsid constructed of three structural proteins, viral proteins 1, 2 and 3 (VP1, 2 and 3). The CPV capsid is arranged according to T=1 icosahedral symmetry with 20 triangular faces related to each other by two-, three- and fivefold rotational axes of symmetry, by nomenclature of Caspar and Klug (CASPAR, D.L., and KLUG, A., 1962) (Figure 1.). The capsid is constructed of 60 copies of capsid protein. A newly produced capsid is comprised of VP2 and VP1, while VP3 is produced in small amounts only in DNA-containing viruses by proteolytic cleavage from VP2 or VP1 (Clinton, G.M., and Hayashi, M., 1976). Proteins VP1 to 3 are identical in sequence except for their N-terminus. The capsid proteins contain a β barrel of 2 loosely connected sheets, the sheets contain 5 and 4 strands named with letters from A to I, while the intervening loops are named by the two strands they connect. The GH loop is remarkably long and makes up the protrusion on the three-fold axis (Tsao, J. et al., 1991) (Figure 2.).

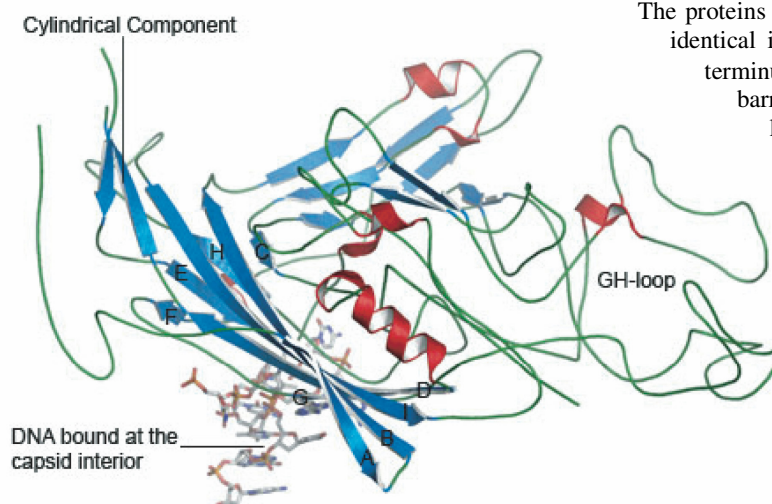


Fig 2. Structure of the CPV capsid protein.

The proteins constructing the CPV capsid are identical in sequence, except for their N-terminus. The core of the protein is a β barrel of nine strands, named with letters from A to I. The DE loop (loop connecting strands D and E) forms a cylindrical component surrounding the cylinder at the five-fold axis of the capsid, while the remarkably long GH loop forms the protrusion on the three-fold axis. An 11 base long segment of DNA is bound at the interior of the capsid. α -helices are shown in red, while β -sheets are shown in dark blue. Green areas represent intervening loops.

The near-atomic three-dimensional structure of several parvoviruses has been determined, including insect densovirus *galleria mellonella* (Simpson, A.A. et al., 1998), porcine parvovirus (PPV) (Simpson, A.A. et al., 2002), minute virus of mouse (MVM) (Llamas-Saiz, A.L. et al., 1997), AAV2 (Xie, Q. et al., 2002), FPV (Agbandje, M. et al., 1993) and empty and full CPV (Chapman, M.S., and Rossmann, M.G., Tsao, J. et al., 1991, Wu, H.,

and Rossmann, M.G., 1993, 1996, Xie, Q., and Chapman, M.S., 1996). Structure of some other parvoviruses has been determined to a lesser resolution (Agbandje, M. et al., 1994, Bruemmer, A. et al., 2005, Walters, R.W. et al., 2004). In general, the structure of these closely related viruses is quite much alike, having cylinder around each five-fold axis, spikes on three-fold axes, depressions on the two-fold axes and canyons surrounding the five-fold axes. The prominence of these features differs between the viruses. X-ray crystallographic data show that in CPV capsid roughly 65% of the five-fold pores are filled with the N-terminal region of 13% of the capsid proteins (Xie, Q., and Chapman, M.S., 1996), although it isn't known which of the proteins occupy this space VP1 is a good candidate (Cotmore, S.F. et al., 1999, Mani, B. et al., 2006).

The canine parvovirus genome is tightly packed in the full capsids, 660 bases of the genome are visible by x-ray crystallography. These 660 bases are loosely bound to the capsid interior in each of the 60 icosahedral asymmetric units and constitute 13% of the genome. The favoured sequence bound by the capsid interior is $X^T/cA^T/cCT^T/c^A/G^A/G^A/G^A X$ (where X is any nucleotide) (Tsao, J. et al., 1991). The CPV virion is remarkably stable; it can tolerate wide temperature and pH changes still retaining its infectivity (Gordon, J.C., and Angrick, E.J., 1986). Yet, it is required to enable some notable feats like the release of the viral genome once it has reached the nucleus of the target cell. Stability versus adaptability can be acquired through series of dynamic changes, triggered by environmental changes or specific interactions with ions or macromolecules.

Merely ~5300 nucleotides long, the (-) stranded ssDNA genome of canine parvovirus contains only two open reading frames (ORF). Separate promoters control the two ORFs, but they terminate at a single polyadenylation site. Each of the genes produces two distinct mRNAs through alternative splicing. Promoter P38 controls the ORF at the 5'-half of the genome that codes for structural proteins, and promoter P4 controls the ORF at the 3'-half that codes for nonstructural proteins (NS1 and 2)(Figure 3.). The genomes of the parvoviruses, including CPV, are unique in structure as they contain terminal repeats, which form T-shaped hairpin structures on both ends of the genome. This structural feature reflects to genome replication since the hairpin on the 3'-end of the genome can act as a primer for synthesis of the complementary strand. (Reed, A.P. et al., 1988)

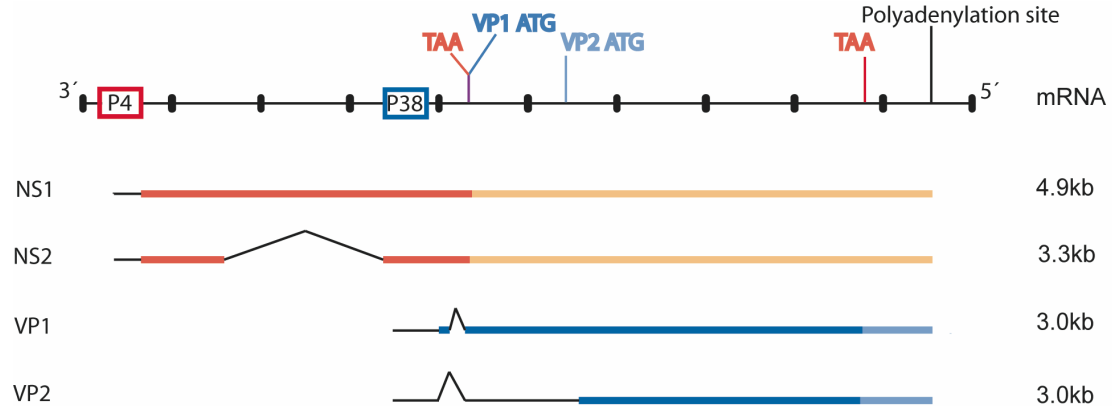


Fig. 3. CPV genome and mRNAs. The single-stranded, ~5300 bases long CPV genome is responsible for the production of a total of five proteins through two open reading frames. Each of the ORFs produce two mRNAs by alternative splicing. The ORFs share the same polyadenylation site but are controlled by different promoters, P4 and P38. The fifth protein is produced post-translationally by proteolytic cleavage in the assembled virus. The CPV genome is displayed in the 3'→5' orientation, mRNAs produced are also shown with the proteins they represent on the left, and the mRNA size on the right. Dark red and blue represent regions translated into proteins, while light colours represent untranslated regions. (Reed, A.P. et al., 1988)

Sneaking by the Cell Membrane

As a virus is in the vicinity of a cell, the first requirement for it to be able to infect the cell is the ability to attach to and penetrate the cell membrane, consequently gaining access to the cytoplasm. The viral entry is a specific process involving interactions between viral proteins and wide variety of molecules on cell surface. The mechanism of entry differs significantly between enveloped and non-enveloped viruses since enveloped viruses tend to be able to exploit direct membrane fusion to enter the cell, whereas non-enveloped viruses are required to resort to more tortuous methods to manage the same (For review see Siczekarski, S.B., and Whittaker, G.R., 2005).

Canine parvovirus uses canine or feline transferrin receptors (TfR) to attach to the cell surface (Hueffer, K. et al., 2003). The apical domain of TfR has been recognized as the site of CPV binding (Palermo, L.M. et al., 2003). When CPV binds to the TfR, it is quickly taken in by dynamin-regulated clathrin-mediated endocytosis and accumulated in late and recycling endosomes (Parker, J.S., and Parrish, C.R., 2000). Rapid intake is a hallmark of

clathrin-mediated endocytosis (Mellman, I., 1996). The regions of TfR binding are located on the shoulders of the three-fold spikes and the edges of the two-fold depressions. In fact, change in only two amino acid residues (VP2 residues 93 and 323) located in these areas is required and sufficient to enable FPV to bind, or prevent CPV from binding, the canine TfR (Parker, J.S., and Parrish, C.R., 1997). Additional amino acid residues affecting the TfR binding has also been revealed, these are also situated in the region of three-fold spikes or edge of two-fold depressions (Hueffer, K. et al., 2003). Although cell susceptibility is largely determined by binding to TfR (Parker, J.S. et al., 2001), this interaction does not guarantee productive infection as some mutations allow capsid binding without leading to infection (Hueffer, K. et al., 2003, Palermo, L.M. et al., 2003). In addition, clathrin-mediated endocytosis is not the only entry route for CPV, since mutations in TfR preventing its association with clathrin through adapter protein 2 did not prevent infection (Hueffer, K. et al., 2004, Palermo, L.M. et al., 2003).

After uptake, CPV is quickly accumulated to perinuclear endosomes and the virus particles remain in these vesicles for several hours (Parker, J.S., and Parrish, C.R., 2000, Suikkanen, S. et al., 2002). The mechanisms underlying the CPV release from the endocytotic vesicles are yet to be discovered. When CPV travels through the endocytotic route, it is exposed to gradually acidifying environment. The acidic treatment is thought to be required for the CPV to effectively escape the endocytotic vesicles (Basak, S., and Turner, H., 1992, Suikkanen, S. et al., 2003b). The unique N-terminal sequence of VP1 contains phospholipase A₂ (PLA₂) activity and is essential for CPV infection as PLA₂ inhibitors prevent infection (Suikkanen, S. et al., 2003b, Zadori, Z. et al., 2001). Infection by PLA₂-mutant virus can be complemented by a wild type virus. The complementation requires packaged genome since empty capsids fail to complement PLA₂-mutant infection (Farr, G.A. et al., 2005). Interestingly, it has been shown that MVM has very inefficient nuclear transport as majority of the virus ends up into lysosomes without showing signs of lysosomal membrane destabilization (Mani, B. et al., 2006).

Towards the Nucleus

As a DNA-virus requiring nuclear enzymes to replicate and transcribe the genome, CPV has to gain access to the nucleus. CPV is released from the endocytotic vesicles to the cytoplasm in the proximity of the nucleus. Subsequently, the viruses are transported to the nucleus by dynein-motor proteins along the microtubule network. The exploitation of the microtubule network and dynein is suggested by the inability of viral capsids to reach the nucleus in the presence of microtubule-depolymerizing agents or anti-dynein antibodies (Suikkanen, S. et al., 2002, Suikkanen, S. et al., 2003a).

Nuclear pore complex (NPC) is a large complex spanning through the nuclear membrane (Maco, B. et al., 2006). NPCs guard the traffic between the nucleoplasm and the cytoplasm. Small macromolecules can diffuse freely through the NPC, whereas large macromolecules need specific, active transport to pass through. Active transport of large macromolecules consumes ATP and requires cytosolic factors like Ran-1 and importins. In addition, the molecule to be transported has to contain a nuclear localization signal (NLS) for it to gain entry into the nucleus. The channel of nuclear pore complex is ~9nm wide, although, the channel of NPC may dilate to suit to the transport of protein-NLS-coated gold particles up to approximately 39nm in diameter (Pante, N., and Kann, M., 2002).

Intact canine parvovirus capsids, ~26nm in diameter, enter the nucleus once injected into the cytoplasm and can be detected by antibodies against intact capsids (Vihinen-Ranta, M. et al., 2002). The nuclear transport of CPV capsids is likely to be controlled by the unique N-terminal sequence of VP1, which, along with its PLA₂ activity, contains a potential classical NLS. This sequence between amino acid residues 4 and 13 is adequate to drive bovine serum albumin into the nucleus and may function as NLS for CPV (Vihinen-Ranta, M. et al., 1997). The VP1 N-terminal sequence is normally buried in the capsid, but becomes exposed during the infection (Vihinen-Ranta, M. et al., 2002). Although the NPC does have the capacity to enable transport of intact CPV capsids, optional mechanism for nuclear entry is through the nuclear envelope, mediated possibly by the VP1 N-terminal PLA₂ activity (Farr, G.A. et al., 2005), this mechanism is suggested by MVM-induced dramatic changes in the nuclear morphology (Cohen, S. et al., 2006).

Viral Replication

It is not yet understood as to how the CPV genome is released from the capsid; one hypothesis is that the genome passes through a channel located in the 5-fold axis of the capsid (Farr, G.A., and Tattersall, P., 2004, Xie, Q., and Chapman, M.S., 1996). Another possibility is the disassembly of the capsid. Evidence favouring the former mechanism is the exposure of 20-30 nucleotides of the 5'-end of the genome, to which NS1 is covalently attached, in newly produced capsids (Cotmore, S.F., and Tattersall, P., 1988). In addition, the T-shaped hairpin structure on the 3'-end of the genome can also be externalized with certain treatments, and can act as a template for DNA polymerase *in vitro* (Cotmore, S.F. et al., 1999, Vihinen-Ranta, M. et al., 2002).

When the CPV genome has been released to the nucleoplasm, it has to wait for the cell to enter S phase, in which the ssDNA genome is converted into double-stranded form. After the genome has been converted into a double-stranded form the P4 promoter is activated and production of proteins NS1 and 2 is initiated. The function of NS2 in CPV infection is unknown; lack of NS2 doesn't impede CPV infection (Wang, D. et al., 1998). Interestingly, NS2 has been proven to affect capsid assembly and translation of viral mRNA of MVM in murine cells (Cotmore, S.F. et al., 1997). NS1, a true jack-of-all-trades, serves multiple purposes including promoter activation, cell cycle arrest, helicase- and nickase-activities and inducement of genome replication and cytopathic effects. A controlled function of NS1 is accomplished by temporal regulation through post-translational modifications, phosphorylation by the members of protein kinase C family, in particular (Nuesch, J.P. et al., 1998, Nuesch, J.P. et al., 2003).

Functions of NS1 of CPV are not thoroughly investigated, but the MVM counterpart is better known. MVM NS1 induces cell cycle arrest in G₁, S and G₂ (Op De Beeck, A. et al., 2001) and recognizes the origin of replication at the 3'-terminal hairpin structure of the parvovirus genome, subsequently assembling replication factors to the site (Willwand, K. et al., 2002). With the help of parvovirus initiation factor, a cellular transcription factor, NS1 executes its nicking activity needed in the process of genome replication (Christensen, J., and Tattersall, P., 2002). NS1 is covalently attached to the 5'-end of the genome in the

nicking process. Both the helicase activity of NS1, and replication fork formation depend on the presence of a cellular single-strand binding protein RPA (replication protein A) (Christensen, J., and Tattersall, P., 2002). NS1 also takes part in viral transcription by activating promoter P38 in concert with cellular transcription factors thus launching the production of capsid proteins (Rhode, S.L.,3rd, 1985b).

Virions begin to assemble as the CPV genome is replicated and capsid proteins are produced at an increasing rate. Both empty and full capsids are produced in canine parvovirus infection. Empty capsids begin accumulating only minutes after the beginning of protein synthesis, but full capsids start to appear only after 1 hour (Yuan, W., and Parrish, C.R., 2001). For some parvoviruses, the capsid assembly has been shown to require other viral components (Cotmore, S.F. et al., 1997). It has been suggested that the genome may be packaged through the cylinder at the five-fold axis (Farr, G.A., and Tattersall, P., 2004), while the precise sequence of events during capsid assembly remain unknown.

The Grand Walkout

Enveloped and non-enveloped viruses differ not only in the entry mechanisms into the cell, but also in method of exiting themselves from the cell. Enveloped viruses take their envelope from some of the membranous structures of the host cell and may be able to bud out of the cell without disrupting the cell (For review see Garoff, H. et al., 1998). Non-enveloped viruses don't have this option and therefore commonly rely on cell lysis as the method of getting out of the cell. Cell lysis may follow even days of accumulation of the virus within the infected cells but is also induced more directly. Very little is known of the exact mechanisms of how viruses directly induce cell death. MVM NS1 induces cytotoxic effects on host cells by mechanisms controlled by the phosphorylation state of the protein (Daeffler, L. et al., 2003, Op De Beeck, A. et al., 2001).

The Pathogenesis

Canine parvovirus has become a worldwide epidemic among dogs, partially due to its resilience of environmental stress. Most dogs are exposed to CPV at some point of their lives, either through vaccination or natural occurrence. Healthy adult dogs are generally rather safe from CPV; however, infection may prove to be lethal for young individuals with insufficient immune defence. Because CPV requires actively growing cells to replicate, it affects primarily lymphoid tissues and rapidly replicating cells of the small intestine (For review see Parrish, C.R., 1995). The common symptoms of CPV infection are diarrhoea, vomiting, destruction of the intestinal lining and reduction in lymphocyte numbers (Figure 4.). In young animals CPV infection affects variety of tissues and may spread to heart, causing myocarditis and possibly death. Other ways by which CPV may cause death are severe dehydration caused by diarrhoea and vomiting and bacterial invasions due to loss of intestinal barrier.

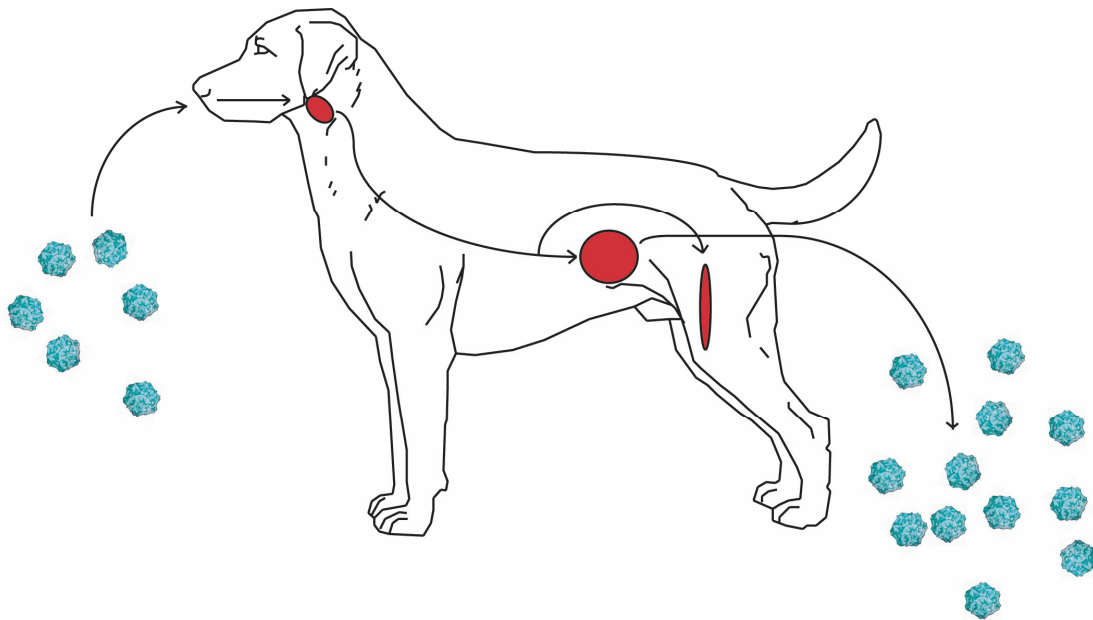


Fig 4. The pathogenesis of CPV. Due to the need of actively dividing cells, CPV often first affects the tonsils. After a few days, the virus spreads to the small intestine and the bone marrow, sites where large numbers of dividing cells are located. Infection of the bone marrow leads to reduction in lymphocyte numbers, whereas consequences of intestinal infection include destruction of the intestinal lining, and therefore diarrhoea and vomiting. Finally, CPV is spread to the environment through the faeces of the infected animal.

Promyelocytic Leukaemia Nuclear Bodies

Cell vs. Virus

Type I and Type II interferon (IFN) responses are considered major pathways for cells to establish defence against viral infection (For review see Goodbourn, S. et al., 2000). Type I interferons include IFN- α and - β while IFN- γ is type II interferon, the two types share no structural homology. IFNs warn neighbouring cells of the impending threat, inducing them to enter an anti-viral state. High level of IFN- α/β expression is observed early in infection by several viruses and is specific for viral infections as it does not occur in infections by other pathogens (For review see Biron, C.A., 1998). The activities of type I interferons are mediated by the JAK-STAT signal transduction pathway and the best-characterized anti-viral effects are induction of (2'-5')-oligoadenylate synthetase (OAS) and the dsRNA-dependent protein kinase (PKR) (For review see Stark, G.R. et al., 1998). (2'-5')-oligoadenylate synthetase activates RNase L and dsRNA-dependent protein kinase phosphorylates translation initiation factor eIF2 (eukaryotic initiation factor 2). Phosphorylation of eIF2 blocks it from recycling from an inactive form and RNase L acts to degrade mRNA, together these events result in general inhibition of protein synthesis. A number of alternative factors are likely to participate in inducing the production of IFN- α/β , one contributing factor is dsRNA, not normally present in normal cells but common result of viral replication (For review see Kaempfer, R., 2003).

Novel anti-viral defence mechanisms have been discovered and they include RNA silencing (Voinnet, O., 2005), the zinc-finger anti-viral protein (Gao, G. et al., 2002) and some members of the tripartite motif (TRIM) protein family (For review see Nisole, S. et al., 2005). Promyelocytic leukaemia (PML) protein is a member of the TRIM family and is proposed to have a role in infection of various viruses (Chee, A.V. et al., 2003, Chelbi-Alix, M.K. et al., 1998, Turelli, P. et al., 2001). PML proteins are mostly found in distinct nuclear bodies called the promyelocytic leukaemia nuclear bodies (PML-NBs) but some isoforms are thought to have cytoplasmic location (Flenghi, L. et al., 1995).

Nuclear Substructure of Mammalian Cell Nucleus

Majority of the mammalian nucleus is dominated by chromatin of varying degrees of condensation and the nucleolus, a prominent nuclear body whose main functions reside in production of ribosomes. Early studies suggested the nucleus to lack significant organization. However, in recent years it has become clear that the nucleus has elaborate organization with several subnuclear organelles specialized for diverse functions (For review see Zimmer, A. et al., 2004) (Figure 5.). Although many of the nuclear processes are known in outstanding detail, knowledge of temporal and spatial interaction of different mechanisms is remarkably poor. The protein components of the subnuclear organelles are often found diffusely in the nucleoplasm as well as in the particular nuclear domains. In many cases, protein exchange between the organelles and the nucleoplasm takes place (Handwerger, K.E. et al., 2003). The significance of the subnuclear organelles may well lie in increasing local concentration of proteins in the nucleoplasm, thus increasing also the efficiency of biochemical processes taking place in the nucleus (Kuthan, H., 2003). Among the most studied and best-known nuclear bodies, other than the nucleolus, are the Cajal bodies (formerly known as Coiled bodies) and the splicing speckles. As both Cajal bodies and the splicing speckles are mainly comprised of molecules taking part in limited number of nuclear processes, it has been relatively straightforward to deduce their potential functions (For review see Lamond, A.I., and Spector, D.L., 2003, For review see Stanek, D., and Neugebauer, K.M., 2006). In contrast, protein constituents of the promyelocytic leukaemia nuclear bodies (PML-NBs) are so diverse, that it has been very difficult to assign any undisputed functions for them. Remarkable new discoveries have been made in recent years concerning the dynamics of the nuclear entities. Some of the subnuclear organelles are found to be dynamic structures exhibiting directional movement (Muratani, M. et al., 2002), while metabolic-energy-dependent movement of yeast chromatin has also been demonstrated (Heun, P. et al., 2001).

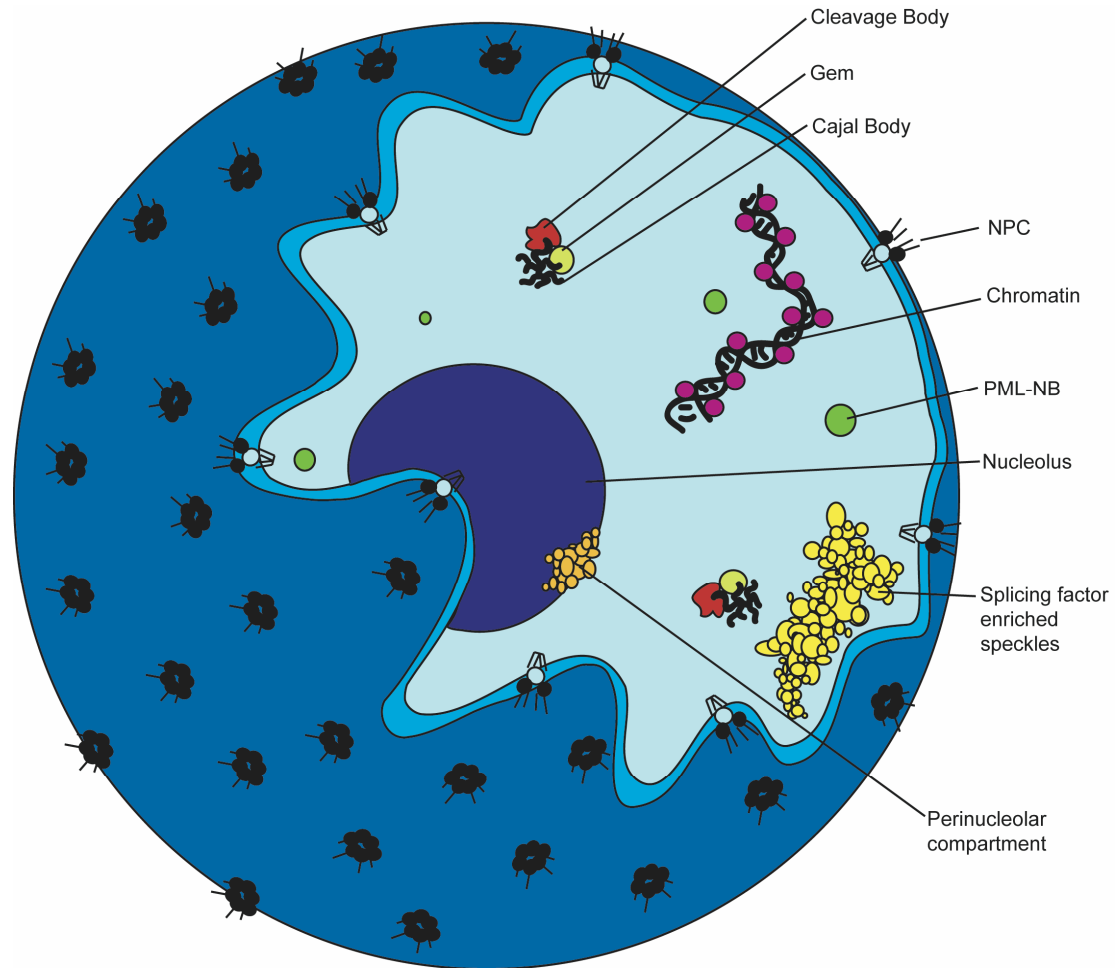


Fig 5. The Nuclear substructure. Many significant substructures can be recognized from the mammalian cell nucleus, only some of them are pictured here. Nucleolus is the most prominent structure found from the nucleus, and has long been thought to be responsible for the production of ribosomes. More novel structures include the splicing speckles, gems, cajal bodies (coiled bodies) and the PML-nuclear bodies. The functions of the novel substructures are under scrutiny, however, it has become clear that the nucleus is far more dynamic and complex than previously thought. Figure adapted from (Spector, D.L., 2001).

PML protein

Promyelocytic leukaemia protein was found in the beginning of the 1990s due to its involvement in Acute Promyelocytic Leukaemia (APL) (Goddard, A.D. et al., 1991, Kakizuka, A. et al., 1991, Kastner, P. et al., 1992, de The, H. et al., 1991). APL is a rare disease associated in 90% of patients with a reciprocal translocation of chromosomes 15 and 17 that entails fusion of PML protein and retinoic acid receptor α (RAR α). PML protein belongs to an extensive family of proteins called the tripartite motif (TRIM) protein

family (For review see Jensen, K. et al., 2001, Moosmann, P. et al., 1996, Reymond, A. et al., 2001). Characteristic feature of the members of the TRIM family is an N-terminal RBCC motif, containing a RING domain (Really Interesting New Gene), one or two B-boxes and a predicted coiled-coil domain. The RING domain is a zinc finger of 40-60 residues that binds two zinc atoms and is found in several proteins with diverse functions, the B-boxes in contrast are specific for the TRIM family. The two B-box domains, B1 and B2, are also zinc-finger domains of approximately 40 residues. The coiled-coil domains are common participants in oligomeric interactions of proteins. All four domains of the RBCC motif are essential for oligomerization or nuclear body formation of PML (Borden, K.L. et al., 1996, Kastner, P. et al., 1992, Shen, T.H. et al., 2006).

Alternative splicing produces several different PML isoforms from nine exons of the ~35kb long PML genomic locus. PML isoforms are divided into seven groups, which are designated as PML I-VII. All of the isoforms are equally expressed (Fagioli, M. et al., 1992). The groups are further divided into sub-groups a/b/c depending on the alternative splicing of exons 4, 5 and 6. Variants b and c lack NLS and thus may exhibit cytoplasmic location (Flenghi, L. et al., 1995). The splicing variants are characterized by differences in the C-terminus as they all share an identical N-terminal RBCC motif. Functional role of the C-terminus is unknown, but isoform specific interaction of PML IV with p53, pRb and histone deacetylase has been demonstrated (Alcalay, M. et al., 1998, Fogal, V. et al., 2000, Wu, W.S. et al., 2001b). Rather little attention has been paid for the different isoforms and their possibly differing roles, which is suggested by the high number of splicing variants and recently discovered isoform specific functions.

Promyelocytic leukaemia protein is found diffusely in the nucleoplasm but it is also required for the formation and integrity of the PML-NBs (Ishov, A.M. et al., 1999, Zhong, S. et al., 2000). First evidence of the role of small ubiquitin like modifier-1 in the localization of PML was found in 1997 (Sternsdorf, T. et al., 1997). Müller, Matunis and Dejean (Muller, S. et al., 1998) showed that unmodified PML was found in the nucleoplasm whereas phosphorylation-dependent covalent attachment of SUMO-1 induces localization of PML into PML-NBs. A recently proposed model for PML-NB formation suggested an important role for a SUMO-binding domain in interaction between

SUMOylated PML-proteins. SUMOylated PML-proteins could mediate binding with others, thus building up into a large complex capable of recruiting additional components (Ishov, A.M. et al., 1999, Shen, T.H. et al., 2006). Intriguingly, PML has also been shown to stimulate hSUMO-1 modification in yeast (Quimby, B.B. et al., 2006). In addition to the important role of SUMO-1 in biology of PML, modification by SUMO-3 has been shown to be essential for nuclear localization of PML (Fu, C. et al., 2005).

PML-NBs – Structure and Dynamics

Promyelocytic leukaemia nuclear bodies are currently identified by the presence of PML protein. Soon after the discovery of the PML protein, it was described to specifically bind to NBs detected as an auto-antigenic target in patients with primary biliary cirrhosis (Dyck, J.A. et al., 1994, Koken, M.H. et al., 1994). PML-NBs are seen as circular structures in electron microscope images and vary in size from 0.3 μm to 1 μm in diameter. Typical mammalian cell nucleus contains 10 to 30 PML-NBs. More than 40 protein species can be detected in PML-NBs, most notably sp100 and retinoblastoma protein (Alcalay, M. et al., 1998, Szostecki, C. et al., 1990). In addition, nascent RNA has been observed to localize in PML-NBs (LaMorte, V.J. et al., 1998). Several studies have revealed the dynamic nature of the components of the PML-NBs (Boisvert, F.M. et al., 2001, Chalkiadaki, A., and Talianidis, I., 2005, Ishov, A.M. et al., 1999). In fluorescence recovery after photobleaching experiments PML and sp100 recover in minutes, while CBP recovers far more quickly (Boisvert, F.M. et al., 2001, Wiesmeijer, K. et al., 2002).

Promyelocytic leukaemia nuclear bodies are dynamic organelles that vary extensively in size, number and mobility (Eskiw, C.H. et al., 2003). The PML-NBs can be divided into three classes based on their mobility. Two of the classes are either immobile or exhibit localized movement (Muratani, M. et al., 2002), which may be merely a result of chromatin dynamics as shown by the similar movement of PML, Cajal and biologically inactive nuclear bodies composed of yellow fluorescent protein-tagged murine Mx1 protein (Gorisch, S.M. et al., 2004). Interestingly, the third class represents highly mobile small PML-NBs, being the first nuclear macromolecular complex proven to move in metabolic-energy-dependent manner (Muratani, M. et al., 2002).

Not only does a subset of PML-NBs scuttle around the nucleus, but the NBs can also respond to various stimuli. PML-NBs have been shown to be under cell cycle specific control and to disperse in response to cellular stress (Eskiw, C.H. et al., 2003, Everett, R.D. et al., 1999). In addition, PML-RAR α , found in APL, is able to sequester the wild-type PML from the PML-NBs in a dominant negative manner; leading to disruption of the PML-NBs (Dyck, J.A. et al., 1994, Koken, M.H. et al., 1994, Weis, K. et al., 1994). However, disruption of NBs by PML-RAR α is reversible since treatment with all-trans retinoic acid (ATRA) or arsenic trioxide (As₂O₃) leads to reappearance of NBs resembling normal PML-NBs (Kakizuka, A. et al., 1991, Koken, M.H. et al., 1994). Heat stress, heavy metal exposure and expression of adenovirus E1A protein all cause the PML-NBs to partially disassemble into smaller PML-containing microstructures. The microstructures appear to bud out of the pre-existing PML-NBs rather than form from diffuse nucleoplasmic PML. During recovery from the stress, the microstructures fuse together and to remnants of the original PML-NBs (Eskiw, C.H. et al., 2003).

In G₂-phase of the cell cycle, cells appear to have substantially increased number of PML-NBs. PML and sp100, which co-localize rather tightly during interphase, seem to separate in early prophase (Everett, R.D. et al., 1999). PML forms mitotic accumulations during mitosis, which may represent a mechanism of partition of the NBs to the daughter cells (Dellaire, G. et al., 2006). A common feature to PML-RAR α -, cellular stress- and cell cycle-induced disruption of PML-NBs is the state of covalent modification by SUMO-1. When not in the PML-NBs, PML protein seems to lack modification by SUMO-1, irrespective of whether it is located in microstructures induced by PML-RAR α or cellular stress or in the mitotic accumulations (Dellaire, G. et al., 2006, Eskiw, C.H. et al., 2003, Muller, S. et al., 1998). In contrast, SUMO-1 modification seems to be commonly associated with reincorporation of PML into the NBs as in treatment of APL cells with ATRA (Muller, S. et al., 1998).

A number of viruses are known to alter the integrity, localization or size of the PML-NBs (Figure 6.). The best-characterized case is herpesvirus HSV-1, whose regulatory protein ICP0 is by far the most studied viral protein related to PML-NB dynamics. ICP0 is capable of disrupting PML-NBs by inducing proteasome-dependent degradation of PML (Chelbi-

Alix, M.K., and de The, H., 1999, Everett, R.D. et al., 1998, Muller, S., and Dejean, A., 1999). ICP0 contains a RING domain, which is essential for its disruptive effect. Adenovirus as well as herpesviruses Human cytomegalovirus (HCMV), Epstein-Barr virus and Human herpesvirus-8 also possess PML-NB-disruptive potential under certain circumstances (For review see Everett, R.D., 2001). In contrast to the disruptive herpes- and adenoviruses, arenaviruses induce relocation of PML to the cytoplasm. The Z protein responsible for this phenomenon is similar to HSV-1 ICP0 as it also contains a RING domain (Borden, K.L. et al., 1998). In comparison to viruses mentioned above, the rabies virus induces deviant PML-NB behaviour. Although the expression of rabies phosphoprotein P sequesters PML into cytoplasm, rabies induces growth of PML-NBs in infected cells. An increase in the size of PML-NBs is induced by one of the four N-terminally truncated P proteins, the P3 (Blondel, D. et al., 2002).

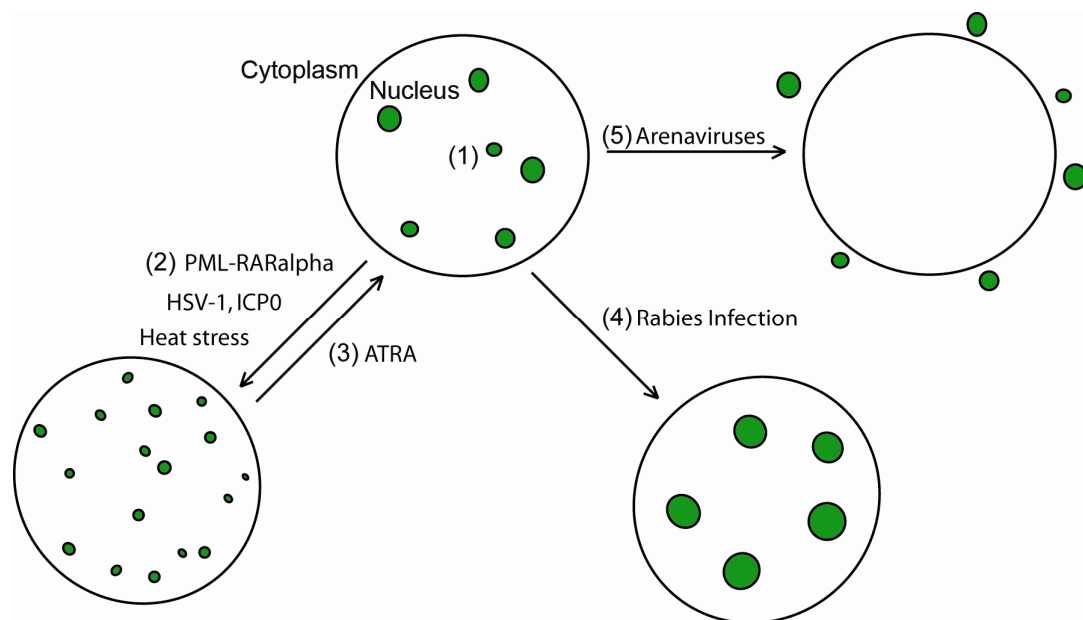


Fig 6. PML-NB Dynamics. PML-NBs are highly dynamic structures affected by many environmental events. (1) PML nuclear bodies in normal, unstressed conditions. (2) Chromosomal translocation creating PML-RAR α fusion protein is a common cause of rare, but severe cancer, the acute promyelocytic leukaemia. The PML-RAR α , as well as heat stress and the ICP0 protein of HSV-1 cause disruption of the PML-NBs into hundreds of smaller structures (Chelbi-Alix, M.K., and de The, H., 1999, Dyck, J.A. et al., 1994, Eskiw, C.H. et al., 2003, Koken, M.H. et al., 1994, Weis, K. et al., 1994). (3) PML-RAR α induced transformation is reversible by treatment with all-trans retinoic acid, which causes reassembly of structures resembling normal PML-NBs (Kakizuka, A. et al., 1991, Koken, M.H. et al., 1994). (4) In contrast to HSV-1 infection, *rabies* virus induces enlargement of the PML-NBs. Interestingly, expression of rabies phosphoprotein P induces effect similar to arenaviruses, whereas the effect observed in infection is induced by a truncated P protein, the P3 (Blondel, D. et al., 2002). (5) The Z protein produced by *arenaviruses* causes relocation of the PML-NBs into the cytoplasm (Borden, K.L. et al., 1998).

Function

A myriad of functions has been assigned to PML-NBs, these encompass e.g.: regulation of transcription (Kiesslich, A. et al., 2002), apoptosis (For review see Bernardi, R., and Pandolfi, P.P., 2003) and cell proliferation (Daniels, M.J. et al., 2004), involvement in DNA repair (Xu, Z.X. et al., 2003, Varadaraj, A. et al., 2007), tumour suppression (For review see Salomoni, P., and Pandolfi, P.P., 2002) and defence against nuclear-replicating viruses (For review see Everett, R.D., 2001, For review see Nisole, S. et al., 2005). In addition, due to the presence of such a high number of various proteins in the PML-NBs it has been proposed that PML-NBs may function as nuclear depots, releasing needed proteins in response to cellular stress (For review see Negorev, D., and Maul, G.G., 2001). Overall, the PML-NB function is still very unclear and under constant debate.

The participation of PML-NBs in tumour suppression was first suggested by the discovery of PML-RAR α in APL. The reciprocal t(15:17) translocation responsible for the fusion of PML and RAR α may produce both RAR α -PML and PML-RAR α (Alcalay, M. et al., 1992). PML-RAR α is able block retinoic acid (RA) induced differentiation by acting as a dominant negative RAR (Damm, K. et al., 1993, Raelson, J.V. et al., 1996, Rousselot, P. et al., 1994). In addition, PML-RAR α disrupts PML-NBs as described above, leading to impediment of the postulated PML-dependent apoptosis (Rogaia, D. et al., 1995). PML-RAR α is able to transform haematopoietic cells *in vitro* and induce acute leukaemia *in vivo* (Altabef, M. et al., 1996, Grisolano, J.L. et al., 1997). PML-RAR α induced transformation is susceptible to treatment with pharmacological doses of ATRA. Not only does ATRA induce reformation of nuclear bodies resembling normal PML-NBs (Kakizuka, A. et al., 1991, Koken, M.H. et al., 1994), but also efficiently eliminates transgenic splenic promyelocytes expressing PML-RAR α *in vitro* (Grisolano, J.L. et al., 1997). While PML-RAR α seems to be the major factor in APL, the RAR α -PML has been shown to enhance the oncogenic effect of PML-RAR α by mechanisms not yet understood (Pollock, J.L. et al., 1999).

The tumour suppressor p53 is an extremely important factor governing the integrity of the genome. The activity of p53 is modified by protein stability and post-translational

modifications. P53^{-/-} cells exhibit resistance to γ irradiation-induced apoptosis; PML^{-/-} cells appear to have the same trait, although to lesser extent (Guo, A. et al., 2000). Co-operation of p53 and PML is indicated not only by the similar consequence of their absence, but also by the impaired induction of p53 target genes in PML^{-/-} cells (Guo, A. et al., 2000). A plausible mechanism of p53 activation by PML is through acetyltransferase CBP, since PML is known to directly interact with it and acetylation is known to activate p53 (Pearson, M. et al., 2000). Remarkably, only PML IV can activate p53 (Fogal, V. et al., 2000) in a PML-NB dependent manner (Pearson, M. et al., 2000). PML is found in nucleolus after DNA damage and is thought to protect p53 by sequestering ubiquitin ligase Mdm2, a negative regulator of p53, there (Bernardi, R. et al., 2004).

While extensive studies support the function of PML in tumour suppression, the role of PML in anti-viral defence is more controversial. Anti-viral activity of the PML-NBs is suggested by the close interaction of several viruses with them. Moreover, expression of PML and some other components of the PML-NBs are enhanced by the type I interferon response, a major cellular anti-viral defence mechanism (For review see Stanek, D., and Neugebauer, K.M., 2006). High expression of PML interferes with replication of several RNA viruses and some DNA viruses (Chee, A.V. et al., 2003, Chelbi-Alix, M.K. et al., 1998, Regad, T. et al., 2001b, Saffert, R.T., and Kalejta, R.F., 2006). While several viruses localize near PML-NBs and have undisputed effect on them, it is not known whether it is the viruses that specifically go to the PML-NBs or vice versa. Majority of the PML-NBs are thought to be relatively immobile. However, some PML-NBs are highly mobile (Muratani, M. et al., 2002). In addition, evidence for the *de novo* emergence of PML-NBs in association of HSV-1 genome has been gathering (Everett, R.D., and Murray, J., 2005). However, the mechanism of association may differ significantly between viruses. Unlike large DNA viruses, smaller viruses like CPV may enter the nucleus intact, thus initial location of their genome depends on the site of uncoating.

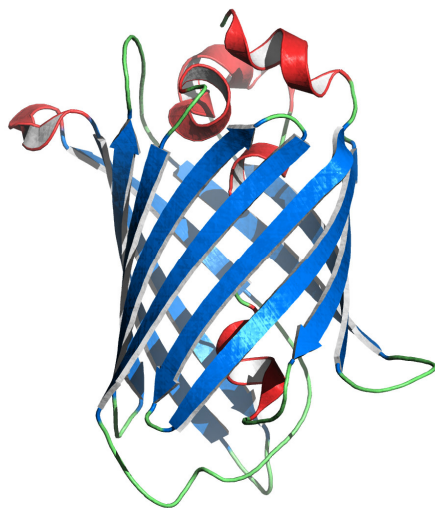
Although increasing evidence supports the role of PML-NBs in viral infections, the mechanism underlying the involvement is unclear. Among many other things, PML-NBs have been linked to repression of gene expression by chromatin remodelling (Wu, W.S. et al., 2001b). This provides an attractive model for the role of PML-NBs in viral infection.

Recent study demonstrates repression of HCMV immediate early gene expression by PML-NB associated protein Daxx and a histone deacetylase (Saffert, R.T., and Kalejta, R.F., 2006). Remarkably, HCMV is able to overcome this anti-viral activity by inducing degradation of Daxx. Another recent study suggests a role for PML-NBs in type I IFN induced cellular response to foreign DNA (Bishop, C.L. et al., 2006). However, not all evidence supports the negative role of PML-NBs in viral infection, as HSV-1 appears to replicate more efficiently when localized near PML-NBs (Sourvinos, G., and Everett, R.D., 2002). In addition, Epstein-Barr virus and Human herpesvirus-8 associate with PML-NBs only upon entry into lytic infection (Bell, P. et al., 2000, Wu, F.Y. et al., 2001a). HSV-1 activates DNA repair pathway during infection, leading to association of ATM and the Mre11/Rad50/Nbs1 complex as well as other proteins involved in DNA repair with the HSV-1 replication compartment (Lilley, C.E. et al., 2005). Interestingly, PML-NBs have also been shown to associate with the Mre11 complex at sites of irradiation induced DNA damage (Carbone, R. et al., 2002).

Confocal Microscopy

Green Fluorescent protein

Green fluorescent protein (GFP) and its variants of different colours have revolutionized the field of fluorescence microscopy. Wild-type GFP found from a jellyfish *Aequorea victoria* emits green light of wavelength 506 nm and has two absorbance maxima at 397 and 475 nm. GFP is an 11-stranded β -barrel approximately 14kDa in size (Figure 7.), the fluorophore is located inside the barrel and forms by cyclization of residues Ser⁶⁵-Tyr⁶⁶-Gly⁶⁷ (Cody, C.W. et al., 1993, Ormo, M. et al., 1996). A number of mutagenesis studies have generated GFP variants with improved properties, including speeding of the fluorophore formation (Zacharias, D.A. et al., 2002), helping GFP to fold correctly in 37°C (Tsien, R.Y., 1998) and converting the two absorbance peaks to a single peak at 489 nm (Delagrave, S. et al., 1995). The improved properties were combined to a single variant, the enhanced GFP (EGFP). In addition, GFP variants with different spectral properties have been produced, these have been named by the colour of the light they emit: BFP for blue (Heim, R. et al., 1994), CFP for cyan (Heim, R. et al., 1994), YFP for yellow (Ormo, M. et al., 1996) and RFP for red (Campbell, R.E. et al., 2002). GFP and its variants are relatively stable and can be genetically linked to variety of proteins; the non-invasive



nature of these fusion proteins has enabled multicolour imaging of different proteins in the same living cells.

Fig 7. The structure of wild-type GFP. The green fluorescent protein is formed by a β -barrel surrounding the fluorophore. The fluorophore forms by cyclization of amino acid residues Ser⁶⁵-Tyr⁶⁶-Gly⁶⁷ located inside the barrel (not seen in the image).

Operational Principle of Confocal Microscope

As early as in mid 1950s, Marvin Minsky made an invention that has had a major impact on fluorescence microscopy, the confocal microscope. However, confocal microscopy became applicable in practice only in the late 1980s due to the development of lasers. In a confocal laser scanning microscope (CLSM) a laser beam is focused to the fluorescent sample by objective lens while two scanning mirrors mounted on motors are responsible for scanning the sample. Fluorescent light and light reflected from the sample are collected by the objective lens, and a beam splitter assorts the fluorescent light from the laser. The fluorescent signal is directed to a detector through a pinhole, which only allows light from certain focal plane to pass. The detector is attached to a computer, which assembles the image. The acquired images are from thin sections of the sample since most of the light from below or above the focal plane is blocked from passing the pinhole to the detector (Figure 8.). Assembling a high-resolution three-dimensional (3D) image is possible after scanning several thin sections of the sample.

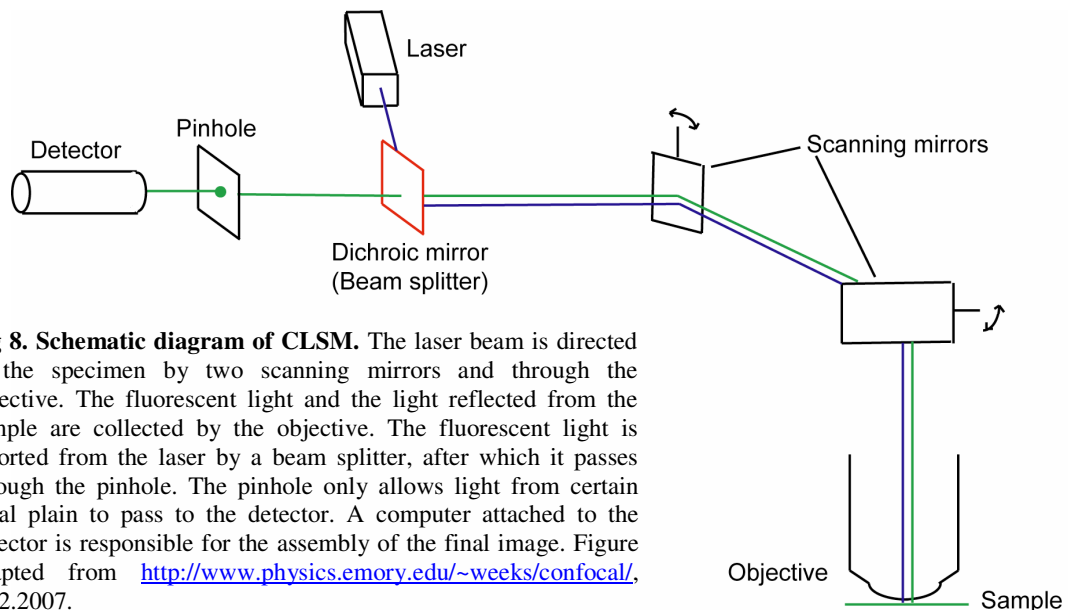


Fig 8. Schematic diagram of CLSM. The laser beam is directed to the specimen by two scanning mirrors and through the objective. The fluorescent light and the light reflected from the sample are collected by the objective. The fluorescent light is assorted from the laser by a beam splitter, after which it passes through the pinhole. The pinhole only allows light from certain focal plain to pass to the detector. A computer attached to the detector is responsible for the assembly of the final image. Figure adapted from <http://www.physics.emory.edu/~weeks/confocal/>, 28.2.2007.

CLSM – a Versatile Tool

The exploitation of confocal microscopy for various research purposes was significantly facilitated with the development of relatively photostable fluorescent proteins and computers powerful enough to process the data acquired. The use of confocal microscope can vary from efforts to observe co-localization of different protein species by acquiring single two- or three-dimensional images of cells to elaborate methods that seek to resolve dynamic properties of proteins in living cells (Goodwin, J.S., and Kenworthy, A.K., 2005, Presley, J.F. et al., 1997, Santangelo, P.J. et al., 2004). Some of the more sophisticated techniques include FRET, FLIP, FRAP and FLIM, fluorescence resonance energy transfer, fluorescence loss in photobleaching, fluorescence recovery after photobleaching and fluorescence lifetime imaging microscopy, respectively.

While defining co-localization of differently labelled proteins by fluorescence microscopy, the proteins may appear to co-localize although considerable distance may separate them. Thus, the images do not provide information of the actual physical interactions of the proteins. The inadequate detection of co-localization is caused by resolution limited to approximately 250 nm due to diffraction of light. Attempts to break this limit have led to development of novel imaging techniques (Kwak, E.S. et al., 2001, de Lange, F. et al., 2001). Fluorescence resonance energy transfer, also called Förster resonance energy transfer, is an ingenious method used to study close interactions of macromolecules or to trace specific nucleic acids in cells. FRET is based on energy transfer between two closely situated fluorophores of overlapping emission and excitation peaks. When the first fluorophore, designated the donor, is excited it can transfer the energy to another fluorophore, the acceptor, instead of releasing the energy as light. If the energy transfer occurs, the acceptor is excited and emits light on its intrinsic wavelength. Energy transfer between the two fluorophores is possible only if they are less than ~10 nm apart; the efficiency of energy transfer diminishes as the distance of the fluorophores increases. FRET has been successfully utilized to study the myosin-actin interaction (Dos Remedios, C.G., and Cooke, R., 1984). In addition, dual FRET molecular beacons, short DNA fragments with stem-loop structure (Sokol, D.L. et al., 1998), have been developed to detect specific nucleic acids with relatively high signal-noise ratio (Santangelo, P.J. et al.,

2004). Although FRET is a phenomenon known for quite some time, a novel approaches for utilizing it continues to be developed, it has been applied for detection of matrix metalloproteinase activity (Yang, J. et al., 2006) and to study structural changes of Ras (Sugawa, M. et al., 2006).

Instead of measuring the intensity of fluorescence, fluorescence lifetime imaging microscopy measures the fluorescence lifetime, defined as the time a probe spends in the excited state before returning to the ground state (Clegg, R.M. et al., 2003). Fluorescence lifetime of a probe is sensitive to the environmental and physical processes that influence the excited state, thus FLIM may detect regional differences in fluorescence lifetimes, suggesting differing local microenvironments (Lakowicz, J.R. et al., 1992). FLIM also provides a method to detect FRET since in the presence of an acceptor the mean lifetime of the donor is shortened (For review see Bastiaens, P.I., and Squire, A., 1999). The fluorescence lifetimes and FRET efficiencies may vary unpredictably, but the effect of FRET may be verified by selectively photobleaching the acceptor. Bleaching the acceptor causes the fluorescence lifetime of the donor to shift to that of an unquenched donor (Chen, Y., and Periasamy, A., 2004). FRET detected using FLIM, has been used to monitor the phosphorylation of epidermal growth factor receptor (Wouters, F.S., and Bastiaens, P.I., 1999). Special equipment for confocal microscope is required in order to make FLIM experiments possible.

Photobleaching signifies permanent loss of fluorophores ability to fluoresce. Photobleaching is induced by exposure of the fluorophore to either repeated cycles of excitation and emission or to laser of high intensity. FLIP and FRAP are closely related techniques that seek to take advantage of this traditionally undesired phenomenon (For review see Koster, M. et al., 2005). EGFP has proved to be very suitable for photobleaching experiments due to its brightness and stability under low-intensity illumination yet fast and irreversible bleaching when illuminated with high intensity (Patterson, G.H. et al., 1997). The resistance of EGFP to low intensity illumination is due to the β -barrel structure, which serves to protect the fluorophore.

Fluorescence loss in photobleaching is commonly used to study continuity of cellular compartments or mobility of proteins within a compartment. FLIP has been used to study e.g. ER-to-Golgi transport (Presley, J.F. et al., 1997), nucleocytoplasmic traffic of Stat1 (Lillemeier, B.F. et al., 2001) and the intranuclear mobility of pre-mRNA splicing factor SF2/ASF (Phair, R.D., and Misteli, T., 2000). FLIP is based on repeated bleaching of desired region of the cell to ensure prevention of fluorescence recovery. The continuous bleaching leads to loss of fluorescence in cellular compartments connected to the bleached region. Loss of fluorescence is only observed if the molecules within these compartments are able to travel to the bleached region, i.e. the molecules are not immobilized. The rate of fluorescence loss depends on extent of communication between the compartments (Figure 9A, B and E). As FLIP and FRAP take slightly different approaches to very similar research problems, they are often utilized in conjunction (Lillemeier, B.F. et al., 2001, Phair, R.D., and Misteli, T., 2000).

FRAP is a technique aiming at monitoring recovery of fluorescence. A rather comprehensive introduction to FRAP is offered by Meyvis et al. (For review see Meyvis, T.K. et al., 1999). In a FRAP experiment a small region of interest is bleached once, causing a dramatic reduction of fluorescence (Figure 9C). According to Meyvis, the optimal amount of bleaching is between 30-70 %. The subsequent rate and extent of fluorescence recovery is monitored. The recovery of fluorescence intensity is a consequence of exchange of bleached and unbleached molecules between the bleached region and the surroundings (Figure 9D). Slow or impaired recovery signifies low mobility of the fluorescently labelled molecules that may be a result viscous environment or variety of diffusion barriers as well as binding of the molecule to macromolecular complexes. In contrast, freely mobile molecules move quickly into the bleached region and the fluorescence is fully recovered (Phair, R.D., and Misteli, T., 2000).

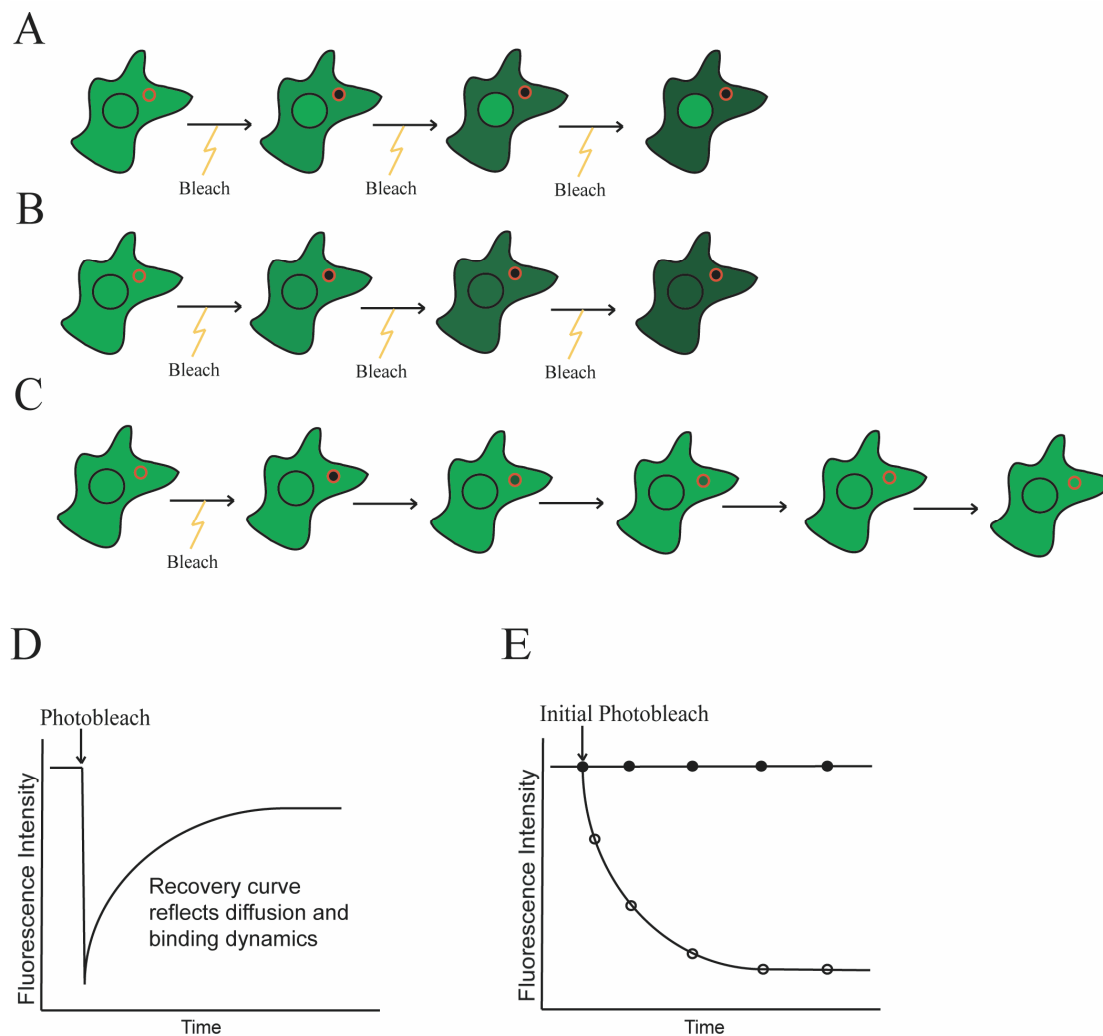


Fig 9. Schematic illustration of FLIP and FRAP techniques. FRAP and FLIP are closely related techniques used to study connectivity of cellular compartments and dynamic properties of cellular proteins. (A, B, E) In a FLIP experiment a region of interest is repeatedly bleached with high intensity laser to prevent recovery of fluorescence in the region. When a protein found throughout the cell is subjected to FLIP, (A) the fluorescence in the cytoplasm fades and nuclear fluorescence remains unaffected if the protein is incapable of nucleo-cytoplasmic shuttling. (B) However, if the protein can escape the nucleus to the cytoplasm, fluorescence in both compartments fade and the rate of nuclear bleaching is dependent on the rate of nuclear export of the protein. (C) In a FRAP experiment, a single laser pulse is used to bleach the region of interest. The possible recovery of fluorescence in the bleached region is followed after the bleaching. Recovery of fluorescence is only observed if the protein is able enter the bleached region. (D, E) Fluorescence intensities detected in FRAP and FLIP experiments, respectively. (D) In FRAP, The rate of fluorescence recovery is dependent on several factors, including diffusion rate, interactions with macromolecular complexes and different kind of diffusional barriers. (E) In FLIP, it is necessary to simultaneously follow the fluorescence intensity of an unbleached cell (curve with filled dots) in order to define bleaching caused by the low intensity imaging. Figure adapted from (Goodwin, J.S., and Kenworthy, A.K., 2005).

FRAP – a Closer Look

The subnuclear organization, particularly the nuclear matrix, has been under vigorous debate for decades (For review see Misteli, T., 2001, For review see Pederson, T., 2000). Recent discoveries by e.g. Houtsmuller et al. and Phair and Misteli have provided new insights into the subnuclear dynamics as they have shown many of the nuclear proteins to move by energy-independent manner (Houtsmuller, A.B. et al., 1999, Phair, R.D., and Misteli, T., 2000). In their studies Houtsmuller and Phair used FRAP to determine the diffusional properties of proteins involved in various nuclear processes. However, long before application of FRAP to intracellular proteins was possible, it was utilized for determining dynamics of membrane-bound molecules (Jacobson, K. et al., 1976). Fluorescence recovery after photobleaching was first developed in the 1970s (Axelrod, D. et al., 1976) but has in past decade gone through a renaissance due to development of CLSM and discovery of GFP. In fact, CLSM is not required for FRAP, although it is the most common choice of equipment. In addition to intracellular events, FRAP can be used to study mobility of molecules in the interstitial spaces of tissues, for example delivery of anticancer therapeutics to tumours (Brown, E.B. et al., 2004).

Two key parameters that can be calculated from FRAP data are the diffusion coefficient D and the mobile fraction M_f . While M_f provides information on the fraction of molecules immobilized by e.g. protein complexes or membrane structures, the diffusion coefficient D describes movement of the molecules due to Brownian motion (i.e. stochastic movement). The basic theory used for quantification of molecular mobility from FRAP data was developed by Axelrod et al. (Axelrod, D. et al., 1976). However, the theory was generated to define two-dimensional lateral diffusion, and thus requires assumptions that are often not met by modern research applications. For this reason, several novel mathematical models for data analysis have been developed (For review see Carrero, G. et al., 2003). Some of the models take a numerical approach to the problem (Wedekind, P. et al., 1996) and are thus laborious for biologists to utilize, while others were generated to be more readily applicable (Braeckmans, K. et al., 2003, Braga, J. et al., 2004). However, even the novel models are best-fit for certain experimental configurations, therefore it is of high importance to choose the model most suitable for the used FRAP set-up, or preferably

consider the model even while designing the experiment. To make matters even more complicated, comparison of the acquired quantitative data is hindered by lack of standards to calibrate the FRAP set-up. Hence, development of GFP-based standard has recently been attempted (Pucadyil, T.J., and Chattopadhyay, A., 2006). The diffusion coefficient and the mobile fraction are not the only numbers calculable from FRAP data. In fact, D is related to the half time of recovery (t_D or $t_{1/2}$, used herein) (Figure 10A), which is comparable between different FRAP studies. However, the importance of diffusion coefficient lies in its capacity to describe the diffusion rate alone, while variation in the $t_{1/2}$ arises from combination of diffusion, binding kinetics (k_{ON}) and unbinding kinetics (k_{OFF}) (Sprague, B.L., and McNally, J.G., 2005).

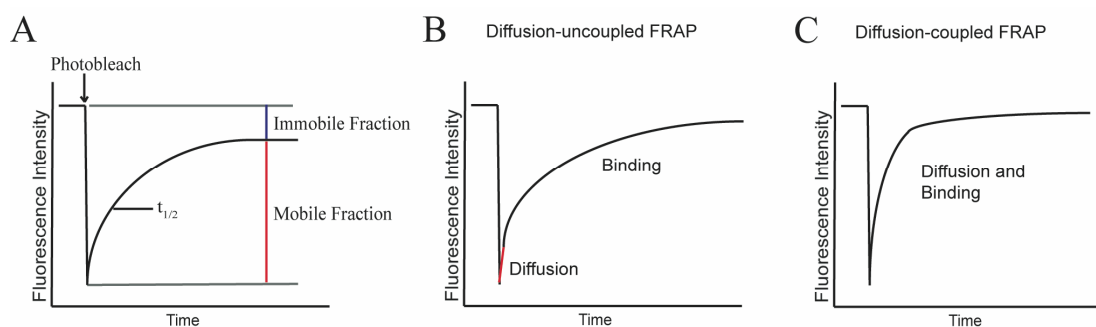


Fig. 10. Analysis of FRAP data. (A) The simplest numbers that can be defined from FRAP data, are the mobile fraction and $t_{1/2}$, the former describes the amount of protein free to diffuse to the bleached area, whereas the latter is defined as the time when fluorescence is half recovered. (B, C) Slow recovery generally suggests participation of binding reactions to FRAP. Although the shape of the curve may give some clue, defining the combination of diffusion and binding properties responsible for a characteristic recovery requires extensive analysis. Figure adapted from (Sprague, B.L., and McNally, J.G., 2005).

As the behaviour of freely diffusing molecules has been extensively analyzed in the long history of FRAP (see above), the analysis of binding properties of proteins has started to attract more and more attention. A number of studies have pursued the representation of mathematical models taking the binding reactions into account (For review see Carrero, G. et al., 2003, Carrero, G. et al., 2004, Sprague, B.L. et al., 2004, For review see Sprague, B.L., and McNally, J.G., 2005). Sprague et al. have recently introduced a straightforward guidelines for interpreting FRAP data (Sprague, B.L. et al., 2004). Participation of binding reactions to the FRAP recovery is generally suggested by slower recovery, the contribution of diffusion to such cases can be deduced by the relationship of two values. Association rate describes the k_{ON} multiplied with the concentration of the molecule, while the inverse

of this number represents the time it takes for a molecule to become bound. In contrast, diffusion rate is the required time for a molecule to diffuse across the bleach spot. If the diffusion rate is fast, as compared to the time required for binding, the recovery can be classified as diffusion-uncoupled. If the opposite is true, the recovery is diffusion-coupled (For review see Sprague, B.L., and McNally, J.G., 2005) (Figure 10B and C).

Quantitative Confocal Microscopy – In Conclusion

As novel microscopic methods have been developed, the role of data analysis has grown significantly (Garcia Penarrubia, P. et al., 2005, Goucher, D.R. et al., 2005, Soltanian-Zadeh, H. et al., 2005). Quantitative confocal microscopy takes many forms (Akita, H. et al., 2004, Choi, H.J. et al., 2005, Price, J.R. et al., 2005) and aims at untangling research problems with ever increasing precision. In some cases, the inadequacy of available mathematical tools for data processing may complicate analysis of the acquired data, while user bias poses another growing problem (Voss, T.C. et al., 2005). As single-cell imaging has become a common practice, concern has risen over the notion of average cell (Levsky, J.M., and Singer, R.H., 2003) due to variation in gene expression among cell population (Elowitz, M.B. et al., 2002). Voss et al. have proposed an unbiased method for selection of transiently transfected cells for imaging. The method is based on cotransfection of cells with plasmids encoding the XFP-tagged protein of interest and a free RFP. The cell to be imaged can be chosen based on expression of RFP without prior knowledge of the expression level of the fusion protein. (Voss, T.C. et al., 2004, Voss, T.C. et al., 2005)

AIM OF THE STUDY

The described studies aimed at:

1. Elucidating the dynamic properties of Promyelocytic leukaemia nuclear bodies in NLFK cells in canine parvovirus infection.
2. Setting up experimental conditions for FRAP experiments.
3. Defining nuclear binding and diffusion properties of PML protein isoform 4 in CPV infection.

Materials and Methods

Sample Preparation

Plasmids

N-terminally tagged EYFP-PML IV, ECFP-PML IV and EYFP-NS1 constructs were utilized in the experiments. The PML-plasmids, previously described (Everett, R.D. et al., 2003), were a generous gift from Everett R.D. (University of Glasgow, Scotland, UK). Jylhävä J. and Niskanen E. (University of Jyväskylä, Finland) produced the pEYFP-NS1 construct (Ihalainen, T.O. et al., 2007). The plasmids were amplified in *Escherichia coli* and purified with the Wizard[®] Plus Midipreps DNA Purification System (Promega) following the protocol provided by the manufacturer.

Cell culture and Transfections

Norden Laboratory Feline Kidney (NLFK) cells, a generous gift from Colin Parrish (Cornell University, Ithaca, New York, USA), were grown and maintained in Dulbecco's modified Eagle's medium (DMEM) supplemented with 10 % inactivated foetal calf serum (FCS, PAA Laboratories GmbH), 1 % L-glutamine, 1 % penicillin-streptomycin and 1 % non-essential amino-acids (Gibco-BRL Life technologies). For transfections, cells were grown either on 60 mm glass-bottom culture dishes (MatTek, USA) or on coverslips in 3 cm culture dishes. The cells were transiently transfected using two different methods, fugene[®]6-reagent (Roche Diagnostic) or electroporation. Transfection by fugene[®]6 was executed according to the instructions of the manufacturer after the cells had been grown for one day. 3 µg and 1,5 µg of plasmid was used for transfection in the 60mm glass-bottom dishes and the 3 cm culture dishes, respectively. 6µl of fugene6-reagent was used per 1,5 µg of plasmid. Transfection by electroporation was executed alongside cell culturing. 400 µl volume of cell suspension was transferred into an electroporation cuvette

(BTX) and desired plasmids were added on the cells. Whether together or alone, 16, 32 and 16 μg of pEYFP-PML, pECFP-PML and pEYFP-NS1 were used, respectively. The cells were electroporated with Electro Cell Manipulator[®] 600 using the following parameters: 500 V Capacitance & resistance, Capacitance 500 μF , Resistance 13 ohm and Charging voltage 130 volts.

If cells were not to be infected by CPV, they were allowed to grow for two days before being imaged by confocal microscope. The cells not imaged live were fixed prior to the imaging in 4% paraformaldehyde (PFA), RT for 20min.

Viruses and Infection

If CPV infection were to be done, it was executed the day following transfection. The growth medium was withdrawn from the culture, and infection was induced with viral medium, MOI 0.5-2. The cells were incubated for 30 minutes at 37°C and 5% CO₂, after which growth medium was added to the cells.

Immunofluorescent Labelling

After being fixed in 4% paraformaldehyde (PFA), RT for 20min, the cells were labelled according to (Vihinen-Ranta, M. et al., 1996) for 1 hour with primary anti-NS1 monoclonal antibody and secondary anti-mouse-alexa-633 antibody. In addition, the cells were embedded in Mowiol-Dabco and imaged by CLSM.

Confocal Microscopy

Equipment

The main instrumentation used to carry out the confocal microscopy experiments, was comprised of Zeiss LSM 510 confocal mounted on a Zeiss Axiovert100M inverted

microscope. The microscope was equipped with heated objective and working stage, heating being controlled by Tempocontrol 37-2 digital (Zeiss). A 63x/1.25 NA Plan-Neofluar oil-immersion objective and a 25mW argon (Ar) laser operated at 60% of the laser power were used in all experiments. In addition to the Zeiss LSM510, Olympus Fluoview FV1000 was used to acquire 2D images.

Performing FRAP Experiments and Analysis of the Data Acquired

FRAP experiments for both live and fixed cells transfected with pEYFP-PML were carried out at 37°C. At first, the cells were placed on the heated stage and the temperature was allowed to settle. The YFP-PML was imaged using 3x zoom and Ar laser at 488 nm with 3 % of the bleaching intensity (~0.18% of the maximum laser power). Three images of the nucleus of a cell were acquired, after which the desired PML-NB was bleached. The bleaching was performed with 100 iterations in a circular ROI (region of interest) of 15 pixels (1.5µm) in diameter. A total of 360 images with 2 second intervals were acquired in a single FRAP experiment. The pinhole was opened to 9.21 airy units and the cell was kept in focus by hand. No image averaging was used.

Tables of the observed fluorescence intensities were generated using LSM510 software provided by Zeiss. ROI was drawn around the bleached PML-NB and the whole nucleus. The fluorescence intensity of the bleached PML-NBs often had to be collected in short periods due to movement of the cell; the ROI was kept constant in shape and size in such cases. The fluorescence intensities of a cell were transferred into a single Microsoft excel file and were subsequently normalized. The normalized fluorescence intensities, $F(t)$, were generated by equation (1) (Goodwin, J.S., and Kenworthy, A.K., 2005).

$$(1) \quad F(t) = I(t) T_i / I_i T(t)$$

Where T_i corresponds to the average fluorescence of the nucleus before bleaching, I_i to the average fluorescence of the bleached region before bleaching, $I(t)$ to the average fluorescence of the bleached region and $T(t)$ to the average fluorescence of the nucleus.

Average fluorescence recovery was determined from cells, whose recovery curves were stable throughout the imaging, i.e. the plane of focus did not drift during imaging. The mobile fraction M_f can be determined according to equation (2).

$$(2) \quad M_f = (F_\infty - F_0) / (F_i - F_0)$$

F_∞ corresponds to the fluorescence intensity at the end of the experiment, while F_0 and F_i , correspond to the fluorescence immediately after and prior to the bleach, respectively.

Movement of the PML-NBs and Analysis of the Data Acquired

As in FRAP experiments, live cells transfected with pEYFP-PML were imaged at 37°C. Prior to the imaging, the cells were placed on the heated working stage and the temperature was allowed to settle. Three-dimensional images were acquired in 8 stacks with pinhole of 1 airy unit for approximately 10 minutes using 3x zoom. Time interval between each image was 7 seconds and a total 90 images was acquired. Image scanning was performed with 488 nm line of the Ar laser with intensity of ~0.18% of the maximum laser power.

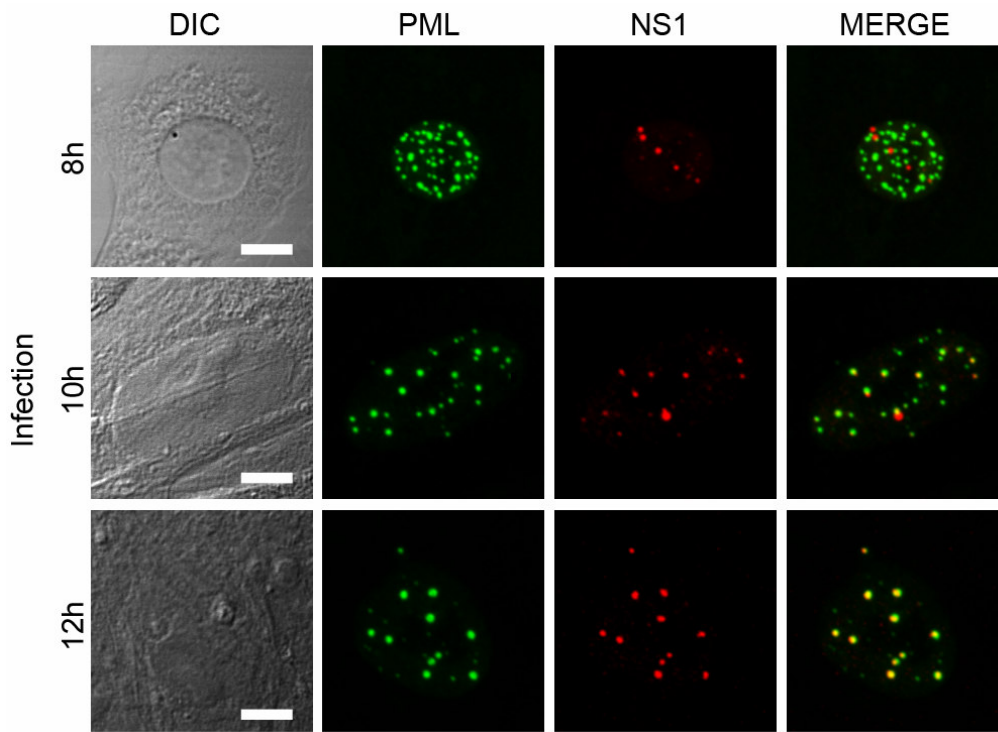
A two-dimensional projection of the acquired image stacks was produced using LSM510 software. The projection images were thereafter processed using ImageJ-software (<http://rsb.info.nih.gov/ij/>, 27.03.2006). ImageJ-plugins downloaded for processing the lsm files and tracking the PML-NB movement were “LSM Reader”, “Manual Tracking” (manual tracker used herein), “Stackreg” and “Turboreg”. Movement of the cell significantly disturbs the determination of movement of single PML-NBs, therefore stackreg was used to eliminate the cellular movement. After processing the images with stackreg, manual tracker was used to define the dynamics of the PML-NBs. The data produced by ImageJ was further processed using Microsoft Office Excel.

RESULTS

Canine Parvovirus Co-localizes with PML-Nuclear Bodies within 12 Hours of Infection

In order to follow viral localization during infection, cells transfected with EYFP-PML were fixed and immunofluorescently labelled for NS1 at various time points after CPV-infection. Subsequently, cells were imaged with confocal laser scanning microscope to follow the accumulations of NS1 in relation to PML-NBs. After eight hours of infection, there was no co-localization detected between labelled NS1-protein and the PML-NBs. However, in later time points the co-localization became more frequent, and finally 12 hours post-infection the two entities showed near-perfect co-localization.

Fig 11. The localization of CPV in the course of infection. Co-localization of CPV with PML-NBs was studied utilizing NLFK cells transfected with pEYFP-PML IV and infected with CPV. The cells were fixed in 4% PFA and immunolabelled with anti-NS1 monoclonal antibody. Finally, the cells were imaged by Olympus Fluoview FV1000. Scalebar 5 μ m.



Canine Parvovirus Appears to Have Very Little Effect on PML Nuclear Body Dynamics upon Infection

After verifying the close apposition of CPV and the PML-NBs late in infection, we wanted to investigate whether CPV infection has any effect on the dynamic properties of the PML-NBs. The number and size of the PML-NBs were determined from confocal images and 4D imaging was utilized to follow their movement. The data was processed with ImageJ and Microsoft office Excel. 24 hours of CPV infection had no effect on the average number of PML-NBs ($p=0.166$). In addition, there were no observed difference in the size of the PML-NBs ($p=0.389$), nor were there significant difference in the average speed (29.9 nm/s and 31.7 nm/s in uninfected and infected cells, respectively, $p=0.113$). Consistent with previous studies, the smallest PML-NBs tended to exhibit the fastest movement, while others showed rather uniform behaviour. Although the average speed of PML-NBs remained unchanged in CPV-infection, the difference in the amount of fast PML-NBs was borderline insignificant ($p=0.052$).

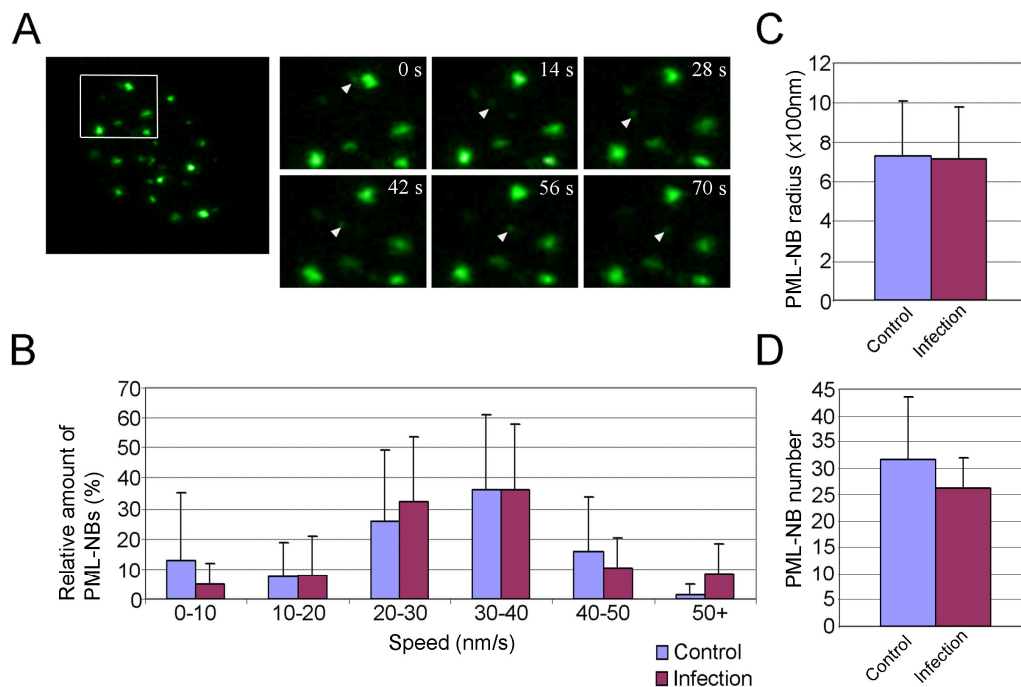


Fig 12. PML-NB dynamics upon CPV infection.

PML-NB dynamics was examined by imaging pEYFP-PML IV-transfected cells with Zeiss LSM510 CLSM. Images were acquired as stacks through the cells; projection of the stacks was used for further analysis. (A) A projection image of an uninfected nucleus, the boxed area is shown magnified with 14 second interval. (B) Distribution of PML-NBs according to average speed. PML-NB speed was determined using Manual Tracking-plugin for ImageJ. Average size (C) and number (D) of PML-NBs.

Dynamic Properties of PML-Protein Remain Unaffected in CPV Infection

Although very mild to no changes were detected in the dynamic properties of the PML-NBs in cells infected by CPV, we wanted to further investigate its possible effect on the PML-protein. We utilized confocal-FRAP to determine the dynamic properties of the PML-protein in normal culture conditions. The half-time of recovery, $t_{1/2}$, was determined as 158.6 seconds, while the mobile fraction was 100%. As the same experiment was carried out for cells 24 hours post-infection, the behaviour of PML-protein was revealed to be effectively identical as compared to control cells.

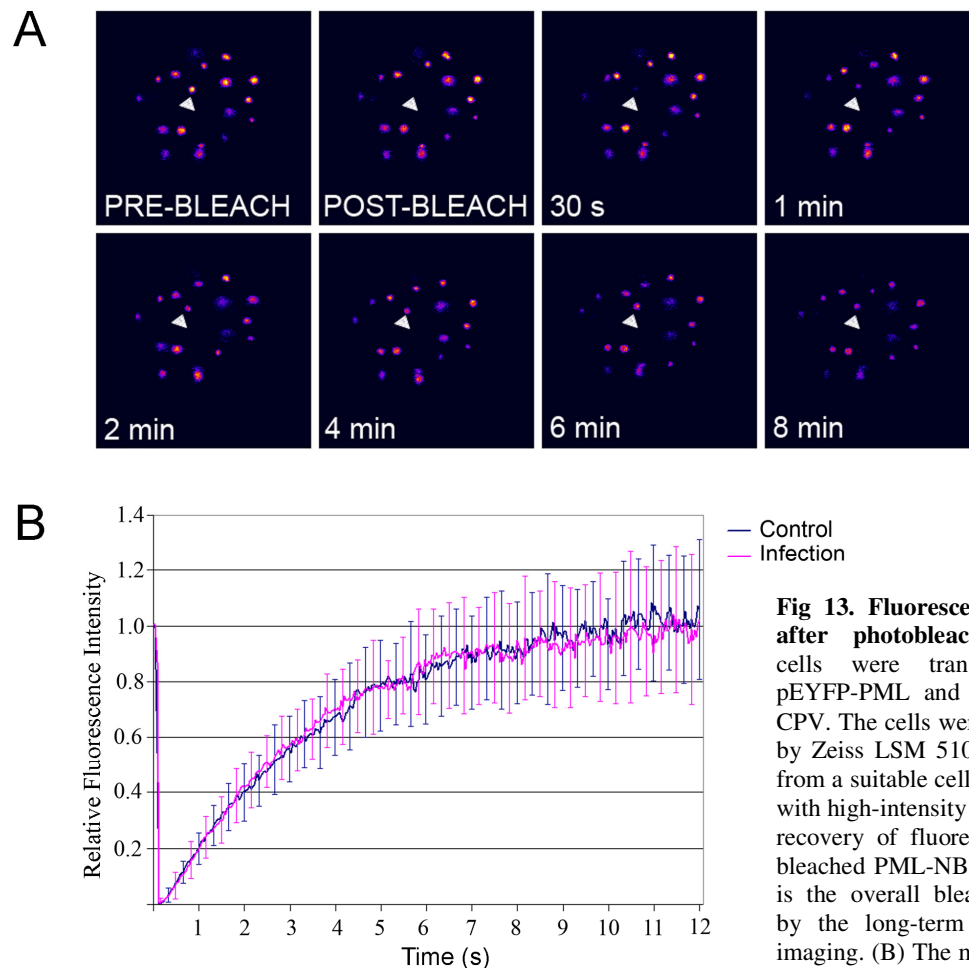


Fig 13. Fluorescence recovery after photobleaching. NLFK cells were transfected with pEYFP-PML and infected with CPV. The cells were imaged live by Zeiss LSM 510. A PML-NB from a suitable cell was bleached with high-intensity laser. (A) The recovery of fluorescence in the bleached PML-NB is evident, as is the overall bleaching caused by the long-term low-intensity imaging. (B) The mobile fraction was shown to be 100%, as the recovery of PML was shown to be very slow, as the half-time of recovery was 158.6 seconds.

relative fluorescence in the bleached PML-NB was eventually fully recovered. The recovery of PML was shown to be very slow, as the half-time of recovery was 158.6 seconds.

DISCUSSION

CPV – PML Interaction

Several viruses, including *Canine parvovirus*, are required to enter the host cell nucleus in order to induce productive infection. However, rather little is known of the interplay between viruses and the nucleus during viral infection. Some viruses are known to interact with the promyelocytic leukaemia nuclear bodies, while for few (namely HSV-I), the manner of interaction is understood in relatively good precision (Everett, R.D., and Murray, J., 2005, Sourvinos, G., and Everett, R.D., 2002). In the described study, we observed and analyzed the dynamic behaviour of both promyelocytic leukaemia nuclear bodies and their defining component, the PML-protein. Since CPV appears to co-localize with PML-NBs during infection, we were interested in determining whether CPV has any profound effect on the dynamics of the PML-NBs, thus bringing some light to the interactions of viruses and nuclear compartments. However, our results are shadowed by suspicion due to the imperfect infectivity of CPV. Not all cells are infected after 24 hour exposure to the virus, thus, some uninfected cells may cause minor distortion to the results since imaging was executed at a single cell level. In addition, as neither the cells nor the infection were synchronized, variation in the stage of cell cycle or infection may have caused additional distortion to the results, especially as PML-NB dynamics have been shown to vary according to the cell cycle (Dellaire, G. et al., 2006, Everett, R.D. et al., 1999).

PML-NBs have been assigned numerous roles, including participation in anti-viral defence, DNA-repair and regulation of transcription and apoptosis. Over-expression of PML-protein leads to increased number and size of PML-NBs and renders the cell resistant to infection by foamy virus (Regad, T. et al., 2001b) and to lesser extent, by HCMV and HSV-1 (Chee, A.V. et al., 2003, Saffert, R.T., and Kalejta, R.F., 2006). As PML has been recognized as an anti-viral effector, it has become clear that numerous viruses disrupt PML-NBs in order to circumvent this activity (Blondel, D. et al., 2002, Borden, K.L. et al., 1998, Chelbi-Alix, M.K., and de The, H., 1999, Everett, R.D. et al., 1998, For review see

Everett, R.D., 2001, Muller, S., and Dejean, A., 1999). Unlike what was expected, CPV appeared to have no effect on PML-NB dynamics, as there was no difference in average number, size or mobility detected. In addition, Canine parvovirus did not affect the properties of PML-protein, displayed by the FRAP experiments. Together these observations support a view of CPV not being susceptible for the anti-viral activity of PML, or circumventing it by other means. As a result, it would be interesting to investigate whether over-expression or lack of PML would have any effect on infectivity of CPV. Since PML promoter contains IFN α -stimulated response element and IFN γ activation sites, PML expression is induced in response to IFNs, making it part of IFN-induced anti-viral response (For review see Regad, T., and Chelbi-Alix, M.K., 2001). Viruses have evolved numerous methods to block IFN-induced events in the infected cell (For review see Regad, T., and Chelbi-Alix, M.K., 2001). Thus, it would be of interest to investigate the IFN-response in NLFK cells to further clarify the mechanism by which CPV is able to avoid it.

Contradicting the anti-viral activity exhibited by the PML, some viruses show increased replication efficiency when localized near PML-NBs (Sourvinos, G., and Everett, R.D., 2002). In addition, localization of some viruses near the PML-NBs marks the transition from lysogenic to lytic infection (Bell, P. et al., 2000, Wu, F.Y. et al., 2001a). As such, PML-NBs has been suggested a role in viral replication. As we observed the co-localization of CPV with PML-NBs by following NS1, viral protein involved in viral genome replication, it should be investigated whether this co-localization coincides with active replication, and whether it is necessary for NS1 function in this regard. Since extensive portion of PML-protein is located diffusely in the nucleoplasm, clarification of the effect of location on PML-protein function would also help solve the significance of PML-NBs for various viruses. In addition, it is of high importance to note the possible isoform-specific functions, as they may partly explain contradictory findings. Although PML-protein is required for formation of PML-NBs (Ishov, A.M. et al., 1999, Zhong, S. et al., 2000), they also contain numerous other components (For review see Matera, A.G., 1999). Thus, localization of CPV NS1 near PML-NBs does not equal direct interaction as there are numerous other potential partners. Co-precipitation, FRET, or related techniques should be utilized in order to study this interaction more closely. Our studies show PML IV-protein to be fully mobile within the nucleus, the recovery was also too slow to be

largely affected by diffusion. Thus, it is evident that whether NS1 and PML IV interact directly or not, CPV infection has no effect on the overall traffic of PML IV between PML-NBs and the nucleoplasm.

Execution of FRAP

Fluorescent recovery after photobleaching is a technique originally developed in the 1970s (Axelrod, D. et al., 1976). After experiencing a renaissance due to development of confocal laser scanning microscope and finding the green fluorescent protein, it has become a powerful tool to determine subcellular dynamics. Our studies showed PML-protein to be fully mobile within the nucleus. However, determination of diffusion coefficient and the binding kinetics (k_{ON} and k_{OFF}) was hindered in our experiments by lack of suitable model for data analysis and poor choice of bleaching intensity. With the increasing amount of specialized applications for FRAP, lack of mathematical models for data analysis has become one of the limiting steps in research. The fluorescence intensity should not be allowed to drop to 0 after bleaching. 30 to 70 % bleaching efficiency would be optimal for purposes of data analysis according to Meyvis et. al. (For review see Meyvis, T.K. et al., 1999). In addition, some background fluorescence should be allowed to enable proper normalization of the data (Goodwin, J.S., and Kenworthy, A.K., 2005).

As PML IV was revealed to be extremely slowly recovering protein, problems resulting from diffusion during bleaching were avoided. However, another problem was faced, as long recovery subdued the experiments vulnerable to focal drift due to temperature changes, air currents etc. (Goodwin, J.S., and Kenworthy, A.K., 2005). We attempted to overcome the problem of focal drift by manually keeping the focus, which in turn, subdued the experiment under human influence. Focal drift could also to some extent be prevented by allowing the temperature of the cell culture dish to equilibrate on the heated working stage of the microscope prior to imaging. Additional problem faced as a consequence of long imaging required by slow recovery of PML, was bleaching due to low intensity imaging. This can best be avoided by decreasing the laser intensity used to acquire post-bleach images, and by increasing detector gain (Goodwin, J.S., and Kenworthy, A.K., 2005).

Finally,

As any good research, this work raised more questions than answered them. In the described study we have shown *canine parvovirus* to be localized near promyelocytic leukaemia nuclear bodies in the course of infection, but to have no effect on their dynamics. Question whether PML-NBs are battling against CPV infection, or whether CPV goes to PML-NBs to enhance or begin replication, remains unanswered. In either case, other components of the PML-NBs than PML protein itself are likely partners for interaction with the virus. Although we were successful in setting up conditions for further FRAP experiments, the light brought to the interactions of viruses and nuclear compartments stayed dim.

REFERENCES

- Agbandje, M., Kajigaya, S., McKenna, R., Young, N.S., and Rossmann, M.G. 1994. The structure of human parvovirus B19 at 8 Å resolution. *Virology*. 203:106-115.
- Agbandje, M., McKenna, R., Rossmann, M.G., Strassheim, M.L., and Parrish, C.R. 1993. Structure determination of feline panleukopenia virus empty particles. *Proteins*. 16:155-171.
- Akita, H., Ito, R., Khalil, I.A., Futaki, S., and Harashima, H. 2004. Quantitative three-dimensional analysis of the intracellular trafficking of plasmid DNA transfected by a nonviral gene delivery system using confocal laser scanning microscopy. *Mol. Ther.* 9:443-451.
- Alcalay, M., Tomassoni, L., Colombo, E., Stoldt, S., Grignani, F., Fagioli, M., Szekely, L., Helin, K., and Pelicci, P.G. 1998. The promyelocytic leukemia gene product (PML) forms stable complexes with the retinoblastoma protein. *Mol. Cell. Biol.* 18:1084-1093.
- Alcalay, M., Zangrilli, D., Fagioli, M., Pandolfi, P.P., Mencarelli, A., Lo Coco, F., Biondi, A., Grignani, F., and Pelicci, P.G. 1992. Expression pattern of the RAR alpha-PML fusion gene in acute promyelocytic leukemia. *Proc. Natl. Acad. Sci. U.S.A.* 89:4840-4844.
- Altabef, M., Garcia, M., Lavau, C., Bae, S.C., Dejean, A., and Samarut, J. 1996. A retrovirus carrying the promyelocyte-retinoic acid receptor PML-RARalpha fusion gene transforms haematopoietic progenitors in vitro and induces acute leukaemias. *EMBO J.* 15:2707-2716.
- Axelrod, D., Koppel, D.E., Schlessinger, J., Elson, E., and Webb, W.W. 1976. Mobility measurement by analysis of fluorescence photobleaching recovery kinetics. *Biophys. J.* 16:1055-1069.
- Barker, I.K., Povey, R.C., and Voigt, D.R. 1983. Response of mink, skunk, red fox and raccoon to inoculation with mink virus enteritis, feline panleukopenia and canine parvovirus and prevalence of antibody to parvovirus in wild carnivores in Ontario. *Can. J. Comp. Med.* 47:188-197.
- Basak, S., and Turner, H. 1992. Infectious entry pathway for canine parvovirus. *Virology*. 186:368-376.
- Bastiaens, P.I., and Squire, A. 1999. Fluorescence lifetime imaging microscopy: spatial resolution of biochemical processes in the cell. *Trends Cell Biol.* 9:48-52.
- Bell, P., Lieberman, P.M., and Maul, G.G. 2000. Lytic but not latent replication of epstein-barr virus is associated with PML and induces sequential release of nuclear domain 10 proteins. *J. Virol.* 74:11800-11810.
- Bernardi, R., and Pandolfi, P.P. 2003. Role of PML and the PML-nuclear body in the control of programmed cell death. *Oncogene*. 22:9048-9057.
- Bernardi, R., Scaglioni, P.P., Bergmann, S., Horn, H.F., Vousden, K.H., and Pandolfi, P.P. 2004. PML regulates p53 stability by sequestering Mdm2 to the nucleolus. *Nat. Cell Biol.* 6:665-672.
- Biron, C.A. 1998. Role of early cytokines, including alpha and beta interferons (IFN-alpha/beta), in innate and adaptive immune responses to viral infections. *Semin. Immunol.* 10:383-390.
- Bishop, C.L., Ramalho, M., Nadkarni, N., May Kong, W., Higgins, C.F., and Krauzewicz, N. 2006. Role for centromeric heterochromatin and PML nuclear bodies in the cellular response to foreign DNA. *Mol. Cell. Biol.* 26:2583-2594.

- Blondel, D., Regad, T., Poisson, N., Pavie, B., Harper, F., Pandolfi, P.P., De The, H., and Chelbi-Alix, M.K. 2002. Rabies virus P and small P products interact directly with PML and reorganize PML nuclear bodies. *Oncogene*. 21:7957-7970.
- Boisvert, F.M., Kruhlak, M.J., Box, A.K., Hendzel, M.J., and Bazett-Jones, D.P. 2001. The transcription coactivator CBP is a dynamic component of the promyelocytic leukemia nuclear body. *J.Cell Biol.* 152:1099-1106.
- Borden, K.L., Campbell Dwyer, E.J., and Salvato, M.S. 1998. An arenavirus RING (zinc-binding) protein binds the oncoprotein promyelocyte leukemia protein (PML) and relocates PML nuclear bodies to the cytoplasm. *J.Virol.* 72:758-766.
- Borden, K.L., Lally, J.M., Martin, S.R., O'Reilly, N.J., Solomon, E., and Freemont, P.S. 1996. In vivo and in vitro characterization of the B1 and B2 zinc-binding domains from the acute promyelocytic leukemia protooncoprotein PML. *Proc.Natl.Acad.Sci.U.S.A.* 93:1601-1606.
- Braeckmans, K., Peeters, L., Sanders, N.N., De Smedt, S.C., and Demeester, J. 2003. Three-dimensional fluorescence recovery after photobleaching with the confocal scanning laser microscope. *Biophys.J.* 85:2240-2252.
- Braga, J., Desterro, J.M., and Carmo-Fonseca, M. 2004. Intracellular macromolecular mobility measured by fluorescence recovery after photobleaching with confocal laser scanning microscopes. *Mol.Biol.Cell.* 15:4749-4760.
- Brown, E.B., Boucher, Y., Nasser, S., and Jain, R.K. 2004. Measurement of macromolecular diffusion coefficients in human tumors. *Microvasc.Res.* 67:231-236.
- Bruemmer, A., Scholari, F., Lopez-Ferber, M., Conway, J.F., and Hewat, E.A. 2005. Structure of an insect parvovirus (Junonia coenia Densovirus) determined by cryo-electron microscopy. *J.Mol.Biol.* 347:791-801.
- Campbell, R.E., Tour, O., Palmer, A.E., Steinbach, P.A., Baird, G.S., Zacharias, D.A., and Tsien, R.Y. 2002. A monomeric red fluorescent protein. *Proc.Natl.Acad.Sci.U.S.A.* 99:7877-7882.
- Carbone, R., Pearson, M., Minucci, S., and Pelicci, P.G. 2002. PML NBs associate with the hMre11 complex and p53 at sites of irradiation induced DNA damage. *Oncogene*. 21:1633-1640.
- Carrero, G., Crawford, E., Hendzel, M.J., and de Vries, G. 2004. Characterizing fluorescence recovery curves for nuclear proteins undergoing binding events. *Bull.Math.Biol.* 66:1515-1545.
- Carrero, G., McDonald, D., Crawford, E., de Vries, G., and Hendzel, M.J. 2003. Using FRAP and mathematical modeling to determine the in vivo kinetics of nuclear proteins. *Methods*. 29:14-28.
- CASPAR, D.L., and KLUG, A. 1962. Physical principles in the construction of regular viruses. *Cold Spring Harb.Symp.Quant.Biol.* 27:1-24.
- Chalkiadaki, A., and Talianidis, I. 2005. SUMO-dependent compartmentalization in promyelocytic leukemia protein nuclear bodies prevents the access of LRH-1 to chromatin. *Mol.Cell.Biol.* 25:5095-5105.
- Chapman, M.S., and Rossmann, M.G. 1996. Structural refinement of the DNA-containing capsid of canine parvovirus using RSRef, a resolution-dependent stereochemically restrained real-space refinement method. *Acta Crystallogr.D Biol.Crystallogr.* 52:129-142.
- Chee, A.V., Lopez, P., Pandolfi, P.P., and Roizman, B. 2003. Promyelocytic leukemia protein mediates interferon-based anti-herpes simplex virus 1 effects. *J.Virol.* 77:7101-7105.
- Chelbi-Alix, M.K., and de The, H. 1999. Herpes virus induced proteasome-dependent degradation of the nuclear bodies-associated PML and Sp100 proteins. *Oncogene*. 18:935-941.

- Chelbi-Alix, M.K., Quignon, F., Pelicano, L., Koken, M.H., and de The, H. 1998. Resistance to virus infection conferred by the interferon-induced promyelocytic leukemia protein. *J.Virol.* 72:1043-1051.
- Chen, Y., and Periasamy, A. 2004. Characterization of two-photon excitation fluorescence lifetime imaging microscopy for protein localization. *Microsc.Res.Tech.* 63:72-80.
- Choi, H.J., Choi, I.H., Kim, T.Y., Cho, N.H., and Choi, H.K. 2005. Three-dimensional visualization and quantitative analysis of cervical cell nuclei with confocal laser scanning microscopy. *Anal.Quant.Cytol.Histol.* 27:174-180.
- Christensen, J., and Tattersall, P. 2002. Parvovirus initiator protein NS1 and RPA coordinate replication fork progression in a reconstituted DNA replication system. *J.Virol.* 76:6518-6531.
- Clegg, R.M., Holub, O., and Gohlke, C. 2003. Fluorescence lifetime-resolved imaging: measuring lifetimes in an image. *Methods Enzymol.* 360:509-542.
- Clinton, G.M., and Hayashi, M. 1976. The parvovirus MVM: a comparison of heavy and light particle infectivity and their density conversion in vitro. *Virology.* 74:57-63.
- Cody, C.W., Prasher, D.C., Westler, W.M., Prendergast, F.G., and Ward, W.W. 1993. Chemical structure of the hexapeptide chromophore of the Aequorea green-fluorescent protein. *Biochemistry.* 32:1212-1218.
- Cohen, S., Behzad, A.R., Carroll, J.B., and Pante, N. 2006. Parvoviral nuclear import: bypassing the host nuclear-transport machinery. *J.Gen.Virol.* 87:3209-3213.
- Cotmore, S.F., D'Abramo, A.M., Jr, Carbonell, L.F., Bratton, J., and Tattersall, P. 1997. The NS2 polypeptide of parvovirus MVM is required for capsid assembly in murine cells. *Virology.* 231:267-280.
- Cotmore, S.F., D'abramo, A.M., Jr, Ticknor, C.M., and Tattersall, P. 1999. Controlled conformational transitions in the MVM virion expose the VP1 N-terminus and viral genome without particle disassembly. *Virology.* 254:169-181.
- Cotmore, S.F., and Tattersall, P. 1988. The NS-1 polypeptide of minute virus of mice is covalently attached to the 5' termini of duplex replicative-form DNA and progeny single strands. *J.Virol.* 62:851-860.
- Daeffler, L., Horlein, R., Rommelaere, J., and Nuesch, J.P. 2003. Modulation of minute virus of mice cytotoxic activities through site-directed mutagenesis within the NS coding region. *J.Virol.* 77:12466-12478.
- Damm, K., Heyman, R.A., Umesono, K., and Evans, R.M. 1993. Functional inhibition of retinoic acid response by dominant negative retinoic acid receptor mutants. *Proc.Natl.Acad.Sci.U.S.A.* 90:2989-2993.
- Daniels, M.J., Marson, A., and Venkitaraman, A.R. 2004. PML bodies control the nuclear dynamics and function of the CHFR mitotic checkpoint protein. *Nat.Struct.Mol.Biol.* 11:1114-1121.
- de Lange, F., Cambi, A., Huijbens, R., de Bakker, B., Rensen, W., Garcia-Parajo, M., van Hulst, N., and Figdor, C.G. 2001. Cell biology beyond the diffraction limit: near-field scanning optical microscopy. *J.Cell.Sci.* 114:4153-4160.
- de The, H., Lavau, C., Marchio, A., Chomienne, C., Degos, L., and Dejean, A. 1991. The PML-RAR alpha fusion mRNA generated by the t(15;17) translocation in acute promyelocytic leukemia encodes a functionally altered RAR. *Cell.* 66:675-684.
- Delagrave, S., Hawtin, R.E., Silva, C.M., Yang, M.M., and Youvan, D.C. 1995. Red-shifted excitation mutants of the green fluorescent protein. *Biotechnology (N.Y).* 13:151-154.
- Dellaire, G., Eskiw, C.H., Dehghani, H., Ching, R.W., and Bazett-Jones, D.P. 2006. Mitotic accumulations of PML protein contribute to the re-establishment of PML nuclear bodies in G1. *J.Cell.Sci.* 119:1034-1042.

Dos Remedios, C.G., and Cooke, R. 1984. Fluorescence energy transfer between probes on actin and probes on myosin. *Biochim.Biophys.Acta.* 788:193-205.

Dyck, J.A., Maul, G.G., Miller, W.H., Jr, Chen, J.D., Kakizuka, A., and Evans, R.M. 1994. A novel macromolecular structure is a target of the promyelocyte-retinoic acid receptor oncoprotein. *Cell.* 76:333-343.

Elowitz, M.B., Levine, A.J., Siggia, E.D., and Swain, P.S. 2002. Stochastic gene expression in a single cell. *Science.* 297:1183-1186.

Eskiw, C.H., Dellaire, G., Mymryk, J.S., and Bazett-Jones, D.P. 2003. Size, position and dynamic behavior of PML nuclear bodies following cell stress as a paradigm for supramolecular trafficking and assembly. *J.Cell.Sci.* 116:4455-4466.

Everett, R.D. 2001. DNA viruses and viral proteins that interact with PML nuclear bodies. *Oncogene.* 20:7266-7273.

Everett, R.D., Freemont, P., Saitoh, H., Dasso, M., Orr, A., Kathoria, M., and Parkinson, J. 1998. The disruption of ND10 during herpes simplex virus infection correlates with the Vmw110- and proteasome-dependent loss of several PML isoforms. *J.Virol.* 72:6581-6591.

Everett, R.D., Lomonte, P., Sternsdorf, T., van Driel, R., and Orr, A. 1999. Cell cycle regulation of PML modification and ND10 composition. *J.Cell.Sci.* 112 (Pt 24):4581-4588.

Everett, R.D., and Murray, J. 2005. ND10 components relocate to sites associated with herpes simplex virus type 1 nucleoprotein complexes during virus infection. *J.Virol.* 79:5078-5089.

Everett, R.D., Sourvinos, G., and Orr, A. 2003. Recruitment of herpes simplex virus type 1 transcriptional regulatory protein ICP4 into foci juxtaposed to ND10 in live, infected cells. *J.Virol.* 77:3680-3689.

Fagioli, M., Alcalay, M., Pandolfi, P.P., Venturini, L., Mencarelli, A., Simeone, A., Acampora, D., Grignani, F., and Pelicci, P.G. 1992. Alternative splicing of PML transcripts predicts coexpression of several carboxy-terminally different protein isoforms. *Oncogene.* 7:1083-1091.

Farr, G.A., and Tattersall, P. 2004. A conserved leucine that constricts the pore through the capsid fivefold cylinder plays a central role in parvoviral infection. *Virology.* 323:243-256.

Farr, G.A., Zhang, L.G., and Tattersall, P. 2005. Parvoviral virions deploy a capsid-tethered lipolytic enzyme to breach the endosomal membrane during cell entry. *Proc.Natl.Acad.Sci.U.S.A.* 102:17148-17153.

Flenghi, L., Fagioli, M., Tomassoni, L., Pileri, S., Gambacorta, M., Pacini, R., Grignani, F., Casini, T., Ferrucci, P.F., and Martelli, M.F. 1995. Characterization of a new monoclonal antibody (PG-M3) directed against the aminoterminal portion of the PML gene product: immunocytochemical evidence for high expression of PML proteins on activated macrophages, endothelial cells, and epithelia. *Blood.* 85:1871-1880.

Fogal, V., Gostissa, M., Sandy, P., Zacchi, P., Sternsdorf, T., Jensen, K., Pandolfi, P.P., Will, H., Schneider, C., and Del Sal, G. 2000. Regulation of p53 activity in nuclear bodies by a specific PML isoform. *EMBO J.* 19:6185-6195.

Fu, C., Ahmed, K., Ding, H., Ding, X., Lan, J., Yang, Z., Miao, Y., Zhu, Y., Shi, Y., Zhu, J., Huang, H., and Yao, X. 2005. Stabilization of PML nuclear localization by conjugation and oligomerization of SUMO-3. *Oncogene.* 24:5401-5413.

Gao, G., Guo, X., and Goff, S.P. 2002. Inhibition of retroviral RNA production by ZAP, a CCCH-type zinc finger protein. *Science.* 297:1703-1706.

- Garcia Penarrubia, P., Ferez Ruiz, X., and Galvez, J. 2005. Quantitative analysis of the factors that affect the determination of colocalization coefficients in dual-color confocal images. *IEEE Trans.Image Process.* 14:1151-1158.
- Garoff, H., Hewson, R., and Opstelten, D.J. 1998. Virus maturation by budding. *Microbiol.Mol.Biol.Rev.* 62:1171-1190.
- Goddard, A.D., Borrow, J., Freemont, P.S., and Solomon, E. 1991. Characterization of a zinc finger gene disrupted by the t(15;17) in acute promyelocytic leukemia. *Science.* 254:1371-1374.
- Goodbourn, S., Didcock, L., and Randall, R.E. 2000. Interferons: cell signalling, immune modulation, antiviral response and virus countermeasures. *J.Gen.Virol.* 81:2341-2364.
- Goodwin, J.S., and Kenworthy, A.K. 2005. Photobleaching approaches to investigate diffusional mobility and trafficking of Ras in living cells. *Methods.* 37:154-164.
- Gordon, J.C., and Angrick, E.J. 1986. Canine parvovirus: environmental effects on infectivity. *Am.J.Vet.Res.* 47:1464-1467.
- Gorisch, S.M., Wachsmuth, M., Itrich, C., Bacher, C.P., Rippe, K., and Lichter, P. 2004. Nuclear body movement is determined by chromatin accessibility and dynamics. *Proc.Natl.Acad.Sci.U.S.A.* 101:13221-13226.
- Goucher, D.R., Wincovitch, S.M., Garfield, S.H., Carbone, K.M., and Malik, T.H. 2005. A quantitative determination of multi-protein interactions by the analysis of confocal images using a pixel-by-pixel assessment algorithm. *Bioinformatics.* 21:3248-3254.
- Grisolano, J.L., Wesselschmidt, R.L., Pelicci, P.G., and Ley, T.J. 1997. Altered myeloid development and acute leukemia in transgenic mice expressing PML-RAR alpha under control of cathepsin G regulatory sequences. *Blood.* 89:376-387.
- Guo, A., Salomoni, P., Luo, J., Shih, A., Zhong, S., Gu, W., and Pandolfi, P.P. 2000. The function of PML in p53-dependent apoptosis. *Nat.Cell Biol.* 2:730-736.
- Handwerger, K.E., Murphy, C., and Gall, J.G. 2003. Steady-state dynamics of Cajal body components in the *Xenopus* germinal vesicle. *J.Cell Biol.* 160:495-504.
- Heim, R., Prasher, D.C., and Tsien, R.Y. 1994. Wavelength mutations and posttranslational autoxidation of green fluorescent protein. *Proc.Natl.Acad.Sci.U.S.A.* 91:12501-12504.
- Heun, P., Laroche, T., Shimada, K., Furrer, P., and Gasser, S.M. 2001. Chromosome dynamics in the yeast interphase nucleus. *Science.* 294:2181-2186.
- Houtsmuller, A.B., Rademakers, S., Nigg, A.L., Hoogstraten, D., Hoeijmakers, J.H., and Vermeulen, W. 1999. Action of DNA repair endonuclease ERCC1/XPF in living cells. *Science.* 284:958-961.
- Hueffer, K., Govindasamy, L., Agbandje-McKenna, M., and Parrish, C.R. 2003. Combinations of two capsid regions controlling canine host range determine canine transferrin receptor binding by canine and feline parvoviruses. *J.Virol.* 77:10099-10105.
- Hueffer, K., Palermo, L.M., and Parrish, C.R. 2004. Parvovirus infection of cells by using variants of the feline transferrin receptor altering clathrin-mediated endocytosis, membrane domain localization, and capsid-binding domains. *J.Virol.* 78:5601-5611.
- Ihalainen, T.O., Niskanen, E.A., Jylhava, J., Turpeinen, T., Rinne, J., Timonen, J., and Vihinen-Ranta, M. 2007. Dynamics and interactions of parvoviral NS1 protein in the nucleus. *Cell.Microbiol.*

- Ishov, A.M., Sotnikov, A.G., Negorev, D., Vladimirova, O.V., Neff, N., Kamitani, T., Yeh, E.T., Strauss, J.F., 3rd, and Maul, G.G. 1999. PML is critical for ND10 formation and recruits the PML-interacting protein daxx to this nuclear structure when modified by SUMO-1. *J. Cell Biol.* 147:221-234.
- Jacobson, K., Derzko, Z., Wu, E.S., Hou, Y., and Poste, G. 1976. Measurement of the lateral mobility of cell surface components in single, living cells by fluorescence recovery after photobleaching. *J. Supramol. Struct.* 5:565(417)-576(428).
- Jensen, K., Shiels, C., and Freemont, P.S. 2001. PML protein isoforms and the RBCC/TRIM motif. *Oncogene.* 20:7223-7233.
- Kaempfer, R. 2003. RNA sensors: novel regulators of gene expression. *EMBO Rep.* 4:1043-1047.
- Kakizuka, A., Miller, W.H., Jr, Umesono, K., Warrell, R.P., Jr, Frankel, S.R., Murty, V.V., Dmitrovsky, E., and Evans, R.M. 1991. Chromosomal translocation t(15;17) in human acute promyelocytic leukemia fuses RAR alpha with a novel putative transcription factor, PML. *Cell.* 66:663-674.
- Kastner, P., Perez, A., Lutz, Y., Rochette-Egly, C., Gaub, M.P., Durand, B., Lanotte, M., Berger, R., and Chambon, P. 1992. Structure, localization and transcriptional properties of two classes of retinoic acid receptor alpha fusion proteins in acute promyelocytic leukemia (APL): structural similarities with a new family of oncoproteins. *EMBO J.* 11:629-642.
- Kiesslich, A., von Mikecz, A., and Hemmerich, P. 2002. Cell cycle-dependent association of PML bodies with sites of active transcription in nuclei of mammalian cells. *J. Struct. Biol.* 140:167-179.
- Koken, M.H., Puvion-Dutilleul, F., Guillemin, M.C., Viron, A., Linares-Cruz, G., Stuurman, N., de Jong, L., Szostecki, C., Calvo, F., and Chomienne, C. 1994. The t(15;17) translocation alters a nuclear body in a retinoic acid-reversible fashion. *EMBO J.* 13:1073-1083.
- Koster, M., Frahm, T., and Hauser, H. 2005. Nucleocytoplasmic shuttling revealed by FRAP and FLIP technologies. *Curr. Opin. Biotechnol.* 16:28-34.
- Kuthan, H. 2003. A mathematical model of single target site location by Brownian movement in subcellular compartments. *J. Theor. Biol.* 221:79-87.
- Kwak, E.S., Kang, T.J., and Vanden Bout, D.A. 2001. Fluorescence lifetime imaging with near-field scanning optical microscopy. *Anal. Chem.* 73:3257-3262.
- Lakowicz, J.R., Szmajcinski, H., Nowaczyk, K., and Johnson, M.L. 1992. Fluorescence lifetime imaging of free and protein-bound NADH. *Proc. Natl. Acad. Sci. U.S.A.* 89:1271-1275.
- Lamond, A.I., and Spector, D.L. 2003. Nuclear speckles: a model for nuclear organelles. *Nat. Rev. Mol. Cell Biol.* 4:605-612.
- LaMorte, V.J., Dyck, J.A., Ochs, R.L., and Evans, R.M. 1998. Localization of nascent RNA and CREB binding protein with the PML-containing nuclear body. *Proc. Natl. Acad. Sci. U.S.A.* 95:4991-4996.
- Levsky, J.M., and Singer, R.H. 2003. Gene expression and the myth of the average cell. *Trends Cell Biol.* 13:4-6.
- Lillemeier, B.F., Koster, M., and Kerr, I.M. 2001. STAT1 from the cell membrane to the DNA. *EMBO J.* 20:2508-2517.
- Lilley, C.E., Carson, C.T., Muotri, A.R., Gage, F.H., and Weitzman, M.D. 2005. DNA repair proteins affect the lifecycle of herpes simplex virus 1. *Proc. Natl. Acad. Sci. U.S.A.* 102:5844-5849.

- Llamas-Saiz, A.L., Agbandje-McKenna, M., Wikoff, W.R., Bratton, J., Tattersall, P., and Rossmann, M.G. 1997. Structure determination of minute virus of mice. *Acta Crystallogr.D Biol.Crystallogr.* 53:93-102.
- Maco, B., Fahrenkrog, B., Huang, N.P., and Aebi, U. 2006. Nuclear pore complex structure and plasticity revealed by electron and atomic force microscopy. *Methods Mol.Biol.* 322:273-288.
- Mani, B., Baltzer, C., Valle, N., Almendral, J.M., Kempf, C., and Ros, C. 2006. Low pH-dependent endosomal processing of the incoming parvovirus minute virus of mice virion leads to externalization of the VP1 N-terminal sequence (N-VP1), N-VP2 cleavage, and uncoating of the full-length genome. *J.Virol.* 80:1015-1024.
- Matera, A.G. 1999. Nuclear bodies: multifaceted subdomains of the interchromatin space. *Trends Cell Biol.* 9:302-309.
- Mellman, I. 1996. Endocytosis and molecular sorting. *Annu.Rev.Cell Dev.Biol.* 12:575-625.
- Meyvis, T.K., De Smedt, S.C., Van Oostveldt, P., and Demeester, J. 1999. Fluorescence recovery after photobleaching: a versatile tool for mobility and interaction measurements in pharmaceutical research. *Pharm.Res.* 16:1153-1162.
- Misteli, T. 2001. Protein dynamics: implications for nuclear architecture and gene expression. *Science.* 291:843-847.
- Moosmann, P., Georgiev, O., Le Douarin, B., Bourquin, J.P., and Schaffner, W. 1996. Transcriptional repression by RING finger protein TIF1 beta that interacts with the KRAB repressor domain of KOX1. *Nucleic Acids Res.* 24:4859-4867.
- Muller, S., and Dejean, A. 1999. Viral immediate-early proteins abrogate the modification by SUMO-1 of PML and Sp100 proteins, correlating with nuclear body disruption. *J.Virol.* 73:5137-5143.
- Muller, S., Matunis, M.J., and Dejean, A. 1998. Conjugation with the ubiquitin-related modifier SUMO-1 regulates the partitioning of PML within the nucleus. *EMBO J.* 17:61-70.
- Muratani, M., Gerlich, D., Janicki, S.M., Gebhard, M., Eils, R., and Spector, D.L. 2002. Metabolic-energy-dependent movement of PML bodies within the mammalian cell nucleus. *Nat.Cell Biol.* 4:106-110.
- Negorev, D., and Maul, G.G. 2001. Cellular proteins localized at and interacting within ND10/PML nuclear bodies/PODs suggest functions of a nuclear depot. *Oncogene.* 20:7234-7242.
- Nisole, S., Stoye, J.P., and Saib, A. 2005. TRIM family proteins: retroviral restriction and antiviral defence. *Nat.Rev.Microbiol.* 3:799-808.
- Nuesch, J.P., Corbau, R., Tattersall, P., and Rommelaere, J. 1998. Biochemical activities of minute virus of mice nonstructural protein NS1 are modulated In vitro by the phosphorylation state of the polypeptide. *J.Virol.* 72:8002-8012.
- Nuesch, J.P., Lachmann, S., Corbau, R., and Rommelaere, J. 2003. Regulation of minute virus of mice NS1 replicative functions by atypical PKClambda in vivo. *J.Virol.* 77:433-442.
- Op De Beeck, A., Sobczak-Thepot, J., Sirma, H., Bourgain, F., Brechot, C., and Caillet-Fauquet, P. 2001. NS1- and minute virus of mice-induced cell cycle arrest: involvement of p53 and p21(cip1). *J.Virol.* 75:11071-11078.
- Ormo, M., Cubitt, A.B., Kallio, K., Gross, L.A., Tsien, R.Y., and Remington, S.J. 1996. Crystal structure of the Aequorea victoria green fluorescent protein. *Science.* 273:1392-1395.

- Palermo, L.M., Hueffer, K., and Parrish, C.R. 2003. Residues in the apical domain of the feline and canine transferrin receptors control host-specific binding and cell infection of canine and feline parvoviruses. *J.Virol.* 77:8915-8923.
- Pante, N., and Kann, M. 2002. Nuclear pore complex is able to transport macromolecules with diameters of about 39 nm. *Mol.Biol.Cell.* 13:425-434.
- Paradiso, P.R., Rhode, S.L., 3rd, and Singer, I.I. 1982. Canine parvovirus: a biochemical and ultrastructural characterization. *J.Gen.Virol.* 62 (Pt 1):113-125.
- Parker, J.S., Murphy, W.J., Wang, D., O'Brien, S.J., and Parrish, C.R. 2001. Canine and feline parvoviruses can use human or feline transferrin receptors to bind, enter, and infect cells. *J.Virol.* 75:3896-3902.
- Parker, J.S., and Parrish, C.R. 2000. Cellular uptake and infection by canine parvovirus involves rapid dynamin-regulated clathrin-mediated endocytosis, followed by slower intracellular trafficking. *J.Virol.* 74:1919-1930.
- Parker, J.S., and Parrish, C.R. 1997. Canine parvovirus host range is determined by the specific conformation of an additional region of the capsid. *J.Virol.* 71:9214-9222.
- Parrish, C.R. 1995. Pathogenesis of feline panleukopenia virus and canine parvovirus. *Baillieres Clin.Haematol.* 8:57-71.
- Patterson, G.H., Knobel, S.M., Sharif, W.D., Kain, S.R., and Piston, D.W. 1997. Use of the green fluorescent protein and its mutants in quantitative fluorescence microscopy. *Biophys.J.* 73:2782-2790.
- Pearson, M., Carbone, R., Sebastiani, C., Cioce, M., Fagioli, M., Saito, S., Higashimoto, Y., Appella, E., Minucci, S., Pandolfi, P.P., and Pelicci, P.G. 2000. PML regulates p53 acetylation and premature senescence induced by oncogenic Ras. *Nature.* 406:207-210.
- Pederson, T. 2000. Half a century of "the nuclear matrix". *Mol.Biol.Cell.* 11:799-805.
- Phair, R.D., and Misteli, T. 2000. High mobility of proteins in the mammalian cell nucleus. *Nature.* 404:604-609.
- Pollock, J.L., Westervelt, P., Kurichety, A.K., Pelicci, P.G., Grisolano, J.L., and Ley, T.J. 1999. A bcr-3 isoform of RARalpha-PML potentiates the development of PML-RARalpha-driven acute promyelocytic leukemia. *Proc.Natl.Acad.Sci.U.S.A.* 96:15103-15108.
- Presley, J.F., Cole, N.B., Schroer, T.A., Hirschberg, K., Zaal, K.J., and Lippincott-Schwartz, J. 1997. ER-to-Golgi transport visualized in living cells. *Nature.* 389:81-85.
- Price, J.R., Aykac, D., Gleason, S.S., Chourey, K., and Liu, Y. 2005. Quantitative comparison of mitotic spindles by confocal image analysis. *J.Biomed.Opt.* 10:44012.
- Pucadyil, T.J., and Chattopadhyay, A. 2006. Confocal fluorescence recovery after photobleaching of green fluorescent protein in solution. *J.Fluoresc.* 16:87-94.
- Quimby, B.B., Yong-Gonzalez, V., Anan, T., Strunnikov, A.V., and Dasso, M. 2006. The promyelocytic leukemia protein stimulates SUMO conjugation in yeast. *Oncogene.* 25:2999-3005.
- Raelson, J.V., Nervi, C., Rosenauer, A., Benedetti, L., Monczak, Y., Pearson, M., Pelicci, P.G., and Miller, W.H., Jr. 1996. The PML/RAR alpha oncoprotein is a direct molecular target of retinoic acid in acute promyelocytic leukemia cells. *Blood.* 88:2826-2832.
- Reaney, D.C. 1982. The evolution of RNA viruses. *Annu.Rev.Microbiol.* 36:47-73.

- Reed, A.P., Jones, E.V., and Miller, T.J. 1988. Nucleotide sequence and genome organization of canine parvovirus. *J.Virol.* 62:266-276.
- Regad, T., and Chelbi-Alix, M.K. 2001a. Role and fate of PML nuclear bodies in response to interferon and viral infections. *Oncogene.* 20:7274-7286.
- Regad, T., Saib, A., Lallemand-Breitenbach, V., Pandolfi, P.P., de The, H., and Chelbi-Alix, M.K. 2001b. PML mediates the interferon-induced antiviral state against a complex retrovirus via its association with the viral transactivator. *EMBO J.* 20:3495-3505.
- Reymond, A., Meroni, G., Fantozzi, A., Merla, G., Cairo, S., Luzi, L., Riganelli, D., Zanaria, E., Messali, S., Cainarca, S., Guffanti, A., Minucci, S., Pelicci, P.G., and Ballabio, A. 2001. The tripartite motif family identifies cell compartments. *EMBO J.* 20:2140-2151.
- Rhode, S.L.,3rd. 1985a. Nucleotide sequence of the coat protein gene of canine parvovirus. *J.Virol.* 54:630-633.
- Rhode, S.L.,3rd. 1985b. trans-Activation of parvovirus P38 promoter by the 76K noncapsid protein. *J.Virol.* 55:886-889.
- Rogaia, D., Grignani, F., Grignani, F., Nicoletti, I., and Pelicci, P.G. 1995. The acute promyelocytic leukemia-specific PML/RAR alpha fusion protein reduces the frequency of commitment to apoptosis upon growth factor deprivation of GM-CSF-dependent myeloid cells. *Leukemia.* 9:1467-1472.
- Rousselot, P., Hardas, B., Patel, A., Guidez, F., Gaken, J., Castaigne, S., Dejean, A., de The, H., Degos, L., and Farzaneh, F. 1994. The PML-RAR alpha gene product of the t(15;17) translocation inhibits retinoic acid-induced granulocytic differentiation and mediated transactivation in human myeloid cells. *Oncogene.* 9:545-551.
- Saffert, R.T., and Kalejta, R.F. 2006. Inactivating a cellular intrinsic immune defense mediated by Daxx is the mechanism through which the human cytomegalovirus pp71 protein stimulates viral immediate-early gene expression. *J.Virol.* 80:3863-3871.
- Salomoni, P., and Pandolfi, P.P. 2002. The role of PML in tumor suppression. *Cell.* 108:165-170.
- Santangelo, P.J., Nix, B., Tsourkas, A., and Bao, G. 2004. Dual FRET molecular beacons for mRNA detection in living cells. *Nucleic Acids Res.* 32:e57.
- Shackelton, L.A., Parrish, C.R., Truyen, U., and Holmes, E.C. 2005. High rate of viral evolution associated with the emergence of carnivore parvovirus. *Proc.Natl.Acad.Sci.U.S.A.* 102:379-384.
- Shen, T.H., Lin, H.K., Scaglioni, P.P., Yung, T.M., and Pandolfi, P.P. 2006. The mechanisms of PML-nuclear body formation. *Mol.Cell.* 24:331-339.
- Sieczkarski, S.B., and Whittaker, G.R. 2005. Viral entry. *Curr.Top.Microbiol.Immunol.* 285:1-23.
- Siegl, G., Bates, R.C., Berns, K.I., Carter, B.J., Kelly, D.C., Kurstak, E., and Tattersall, P. 1985. Characteristics and taxonomy of Parvoviridae. *Intervirology.* 23:61-73.
- Simpson, A.A., Chipman, P.R., Baker, T.S., Tijssen, P., and Rossmann, M.G. 1998. The structure of an insect parvovirus (*Galleria mellonella* densovirus) at 3.7 Å resolution. *Structure.* 6:1355-1367.
- Simpson, A.A., Hebert, B., Sullivan, G.M., Parrish, C.R., Zadori, Z., Tijssen, P., and Rossmann, M.G. 2002. The structure of porcine parvovirus: comparison with related viruses. *J.Mol.Biol.* 315:1189-1198.
- Sokol, D.L., Zhang, X., Lu, P., and Gewirtz, A.M. 1998. Real time detection of DNA:RNA hybridization in living cells. *Proc.Natl.Acad.Sci.U.S.A.* 95:11538-11543.

- Soltanian-Zadeh, H., Shahrokni, A., Khalighi, M.M., Zhang, Z.G., Zoroofi, R.A., Maddah, M., and Chopp, M. 2005. 3-D quantification and visualization of vascular structures from confocal microscopic images using skeletonization and voxel-coding. *Comput.Biol.Med.* 35:791-813.
- Sourvinos, G., and Everett, R.D. 2002. Visualization of parental HSV-1 genomes and replication compartments in association with ND10 in live infected cells. *EMBO J.* 21:4989-4997.
- Spector, D.L. 2001. Nuclear domains. *J.Cell.Sci.* 114:2891-2893.
- Sprague, B.L., and McNally, J.G. 2005. FRAP analysis of binding: proper and fitting. *Trends Cell Biol.* 15:84-91.
- Sprague, B.L., Pego, R.L., Stavreva, D.A., and McNally, J.G. 2004. Analysis of binding reactions by fluorescence recovery after photobleaching. *Biophys.J.* 86:3473-3495.
- Stanek, D., and Neugebauer, K.M. 2006. The Cajal body: a meeting place for spliceosomal snRNPs in the nuclear maze. *Chromosoma.* 115:343-354.
- Stark, G.R., Kerr, I.M., Williams, B.R., Silverman, R.H., and Schreiber, R.D. 1998. How cells respond to interferons. *Annu.Rev.Biochem.* 67:227-264.
- Sternsdorf, T., Jensen, K., and Will, H. 1997. Evidence for covalent modification of the nuclear dot-associated proteins PML and Sp100 by PIC1/SUMO-1. *J.Cell Biol.* 139:1621-1634.
- Sugawa, M., Arai, Y., Iwane, A.H., Ishii, Y., and Yanagida, T. 2006. Single molecule FRET for the study on structural dynamics of biomolecules. *BioSystems.*
- Suikkanen, S., Aaltonen, T., Nevalainen, M., Valilehto, O., Lindholm, L., Vuento, M., and Vihinen-Ranta, M. 2003a. Exploitation of microtubule cytoskeleton and dynein during parvoviral traffic toward the nucleus. *J.Virol.* 77:10270-10279.
- Suikkanen, S., Antila, M., Jaatinen, A., Vihinen-Ranta, M., and Vuento, M. 2003b. Release of canine parvovirus from endocytic vesicles. *Virology.* 316:267-280.
- Suikkanen, S., Saajarvi, K., Hirsimaki, J., Valilehto, O., Reunanen, H., Vihinen-Ranta, M., and Vuento, M. 2002. Role of recycling endosomes and lysosomes in dynein-dependent entry of canine parvovirus. *J.Virol.* 76:4401-4411.
- Szostecki, C., Guldner, H.H., Netter, H.J., and Will, H. 1990. Isolation and characterization of cDNA encoding a human nuclear antigen predominantly recognized by autoantibodies from patients with primary biliary cirrhosis. *J.Immunol.* 145:4338-4347.
- Truyen, U., Evermann, J.F., Vieler, E., and Parrish, C.R. 1996. Evolution of canine parvovirus involved loss and gain of feline host range. *Virology.* 215:186-189.
- Truyen, U., and Parrish, C.R. 1992. Canine and feline host ranges of canine parvovirus and feline panleukopenia virus: distinct host cell tropisms of each virus in vitro and in vivo. *J.Virol.* 66:5399-5408.
- Tsao, J., Chapman, M.S., Agbandje, M., Keller, W., Smith, K., Wu, H., Luo, M., Smith, T.J., Rossmann, M.G., and Compans, R.W. 1991. The three-dimensional structure of canine parvovirus and its functional implications. *Science.* 251:1456-1464.
- Tsien, R.Y. 1998. The green fluorescent protein. *Annu.Rev.Biochem.* 67:509-544.
- Turelli, P., Doucas, V., Craig, E., Mangeat, B., Klages, N., Evans, R., Kalpana, G., and Trono, D. 2001. Cytoplasmic recruitment of INI1 and PML on incoming HIV preintegration complexes: interference with early steps of viral replication. *Mol.Cell.* 7:1245-1254.

- Varadaraj, A., Dovey, C., Laredj, L., Ferguson, B., Alexander, C., Lubben, N., Wyllie, A., and Rich, T. 2007. Evidence for the receipt of DNA damage stimuli by PML nuclear domains. *J.Pathol.*
- Vihinen-Ranta, M., Kakkola, L., Kalela, A., Vilja, P., and Vuento, M. 1997. Characterization of a nuclear localization signal of canine parvovirus capsid proteins. *Eur.J.Biochem.* 250:389-394.
- Vihinen-Ranta, M., Lindfors, E., Heiska, L., Veijalainen, P., and Vuento, M. 1996. Detection of canine parvovirus antigens with antibodies to synthetic peptides. *Arch.Virol.* 141:1741-1748.
- Vihinen-Ranta, M., Wang, D., Weichert, W.S., and Parrish, C.R. 2002. The VP1 N-terminal sequence of canine parvovirus affects nuclear transport of capsids and efficient cell infection. *J.Virol.* 76:1884-1891.
- Voinnet, O. 2005. Induction and suppression of RNA silencing: insights from viral infections. *Nat.Rev.Genet.* 6:206-220.
- Voss, T.C., Demarco, I.A., Booker, C.F., and Day, R.N. 2004. Computer-assisted image analysis protocol that quantitatively measures subnuclear protein organization in cell populations. *BioTechniques.* 36:240-247.
- Voss, T.C., Demarco, I.A., Booker, C.F., and Day, R.N. 2005. Quantitative methods to analyze subnuclear protein organization in cell populations with varying degrees of protein expression. *BioTechniques.* 10:024011.
- Walters, R.W., Agbandje-McKenna, M., Bowman, V.D., Moninger, T.O., Olson, N.H., Seiler, M., Chiorini, J.A., Baker, T.S., and Zabner, J. 2004. Structure of adeno-associated virus serotype 5. *J.Virol.* 78:3361-3371.
- Wang, D., Yuan, W., Davis, I., and Parrish, C.R. 1998. Nonstructural protein-2 and the replication of canine parvovirus. *Virology.* 240:273-281.
- Wedekind, P., Kubitscheck, U., Heinrich, O., and Peters, R. 1996. Line-scanning microphotolysis for diffraction-limited measurements of lateral diffusion. *Biophys.J.* 71:1621-1632.
- Weis, K., Rambaud, S., Lavau, C., Jansen, J., Carvalho, T., Carmo-Fonseca, M., Lamond, A., and Dejean, A. 1994. Retinoic acid regulates aberrant nuclear localization of PML-RAR alpha in acute promyelocytic leukemia cells. *Cell.* 76:345-356.
- Wiesmeijer, K., Molenaar, C., Bekeer, I.M., Tanke, H.J., and Dirks, R.W. 2002. Mobile foci of Sp100 do not contain PML: PML bodies are immobile but PML and Sp100 proteins are not. *J.Struct.Biol.* 140:180-188.
- Willwand, K., Moroianu, A., Horlein, R., Stremmel, W., and Rommelaere, J. 2002. Specific interaction of the nonstructural protein NS1 of minute virus of mice (MVM) with [ACCA]₂ motifs in the centre of the right-end MVM DNA palindrome induces hairpin-primed viral DNA replication. *J.Gen.Virol.* 83:1659-1664.
- Wouters, F.S., and Bastiaens, P.I. 1999. Fluorescence lifetime imaging of receptor tyrosine kinase activity in cells. *Curr.Biol.* 9:1127-1130.
- Wu, F.Y., Ahn, J.H., Alcendor, D.J., Jang, W.J., Xiao, J., Hayward, S.D., and Hayward, G.S. 2001a. Origin-independent assembly of Kaposi's sarcoma-associated herpesvirus DNA replication compartments in transient cotransfection assays and association with the ORF-K8 protein and cellular PML. *J.Virol.* 75:1487-1506.
- Wu, H., and Rossmann, M.G. 1993. The canine parvovirus empty capsid structure. *J.Mol.Biol.* 233:231-244.
- Wu, W.S., Vallian, S., Seto, E., Yang, W.M., Edmondson, D., Roth, S., and Chang, K.S. 2001b. The growth suppressor PML represses transcription by functionally and physically interacting with histone deacetylases. *Mol.Cell.Biol.* 21:2259-2268.

- Xie, Q., Bu, W., Bhatia, S., Hare, J., Somasundaram, T., Azzi, A., and Chapman, M.S. 2002. The atomic structure of adeno-associated virus (AAV-2), a vector for human gene therapy. *Proc.Natl.Acad.Sci.U.S.A.* 99:10405-10410.
- Xie, Q., and Chapman, M.S. 1996. Canine parvovirus capsid structure, analyzed at 2.9 Å resolution. *J.Mol.Biol.* 264:497-520.
- Xu, Z.X., Timanova-Atanasova, A., Zhao, R.X., and Chang, K.S. 2003. PML colocalizes with and stabilizes the DNA damage response protein TopBP1. *Mol.Cell.Biol.* 23:4247-4256.
- Yang, J., Zhang, Z., Lin, J., Lu, J., Liu, B.F., Zeng, S., and Luo, Q. 2006. Detection of MMP activity in living cells by a genetically encoded surface-displayed FRET sensor. *Biochim.Biophys.Acta.*
- Yuan, W., and Parrish, C.R. 2001. Canine parvovirus capsid assembly and differences in mammalian and insect cells. *Virology.* 279:546-557.
- Zacharias, D.A., Violin, J.D., Newton, A.C., and Tsien, R.Y. 2002. Partitioning of lipid-modified monomeric GFPs into membrane microdomains of live cells. *Science.* 296:913-916.
- Zadori, Z., Szelei, J., Lacoste, M.C., Li, Y., Gariépy, S., Raymond, P., Allaire, M., Nabi, I.R., and Tijssen, P. 2001. A viral phospholipase A2 is required for parvovirus infectivity. *Dev.Cell.* 1:291-302.
- Zhong, S., Muller, S., Ronchetti, S., Freemont, P.S., Dejean, A., and Pandolfi, P.P. 2000. Role of SUMO-1-modified PML in nuclear body formation. *Blood.* 95:2748-2752.
- Zimber, A., Nguyen, Q.D., and Gespach, C. 2004. Nuclear bodies and compartments: functional roles and cellular signalling in health and disease. *Cell.Signal.* 16:1085-1104.